$^{20}Ne(\alpha,^{12}C)^{12}C$ reaction

Charles A. Davis*
University of Wisconsin, Madison, Wisconsin 53706
(Received 23 March 1981)

Cross sections at up to 15 angles and in 10 keV steps between $13.4 < E_\alpha < 20.8$ MeV for both $^{20}Ne(\alpha,^{12}C)^{12}C$ and $^{20}Ne(\alpha,\alpha_i)^{20}Ne$ are reported. The absolute cross sections indicate (via detailed balance) serious systematic errors in published $^{12}C(^{12}C,\alpha)^{20}Ne$ cross sections. The data show much resonant structure and, using the $^{20}Ne(\alpha,^{12}C)^{12}C$ data, J^π assignments and extracted resonant parameters for 55 states in ^{24}Mg can be found, only 10 of which had been assigned previously. The systematics of these states seem more consistent with the Friedman-Goebel barrier top resonances than with "quasimolecular" resonances. The alpha scattering data show little correlation with the $^{20}Ne(\alpha,^{12}C)^{12}C$ channel.

[NUCLEAR REACTIONS $^{20}Ne(\alpha,^{12}C)^{12}C$; measured $\sigma(E,\theta)$ at up to 15 angles. $^{20}Ne(\alpha,\alpha_0\alpha_1\alpha_2\alpha_3\alpha_4\alpha_5\alpha_6\alpha_{10}\alpha_{11}\alpha_{13})$ measured $\sigma(E,\theta)$ at one or two angles. $13.4 < E_\alpha$ (MeV) < 20.8, $\Delta E_\alpha = 10$ keV. Deduced ^{24}Mg level parameters J^π, Γ, $(\Gamma_\alpha\Gamma_c)^{1/2}/\Gamma$, E_r. Ne gas target.]

I. INTRODUCTION

The $^{12}C + ^{12}C$ reaction first suggested quasimolecular heavy ion resonances (in approximately 1960),[1,2] and since that time this reaction has perhaps absorbed more experimental and theoretical effort[3–17] than any other heavy ion reaction. One of the better studied[5–16] exit channels is $^{12}C(^{12}C,\alpha)^{20}Ne$. The same information is of course available from the inverse reaction $^{20}Ne(\alpha,^{12}C)^{12}C$. The inverse reaction, except for some early work in Copenhagen,[3,4] has largely been ignored, although there are intrinsic advantages to this approach if one desires accurate absolute cross sections and high energy resolution. The intrinsic advantage relevant to absolute cross section determinations is the accurately known charge state of the alpha particle compared to the poorly known mean charge state of the ^{12}C projectile after emerging from the target. In addition, the large straggling of a ^{12}C particle, both in the stripping foil of the tandem and in the target, limits the energy resolution to typically 50 keV compared to ~ 3 keV for an alpha particle. A great number of other channels from $^{12}C + ^{12}C$ reactions have now been investigated. Several review articles have appeared on the subject.[18–23]

The present paper reports absolute cross sections at up to 15 angles of the $^{20}Ne(\alpha,^{12}C)^{12}C$ reaction. The data cover an excitation energy range of the compound nucleus ^{24}Mg between $20.5 \leq E_x \leq 26.6$ MeV. The center of mass energy steps were usually 8.3 keV, but over part of the region they were 16.7 keV. The 10 000 cross sections permitted a Legendre polynomial analysis and extraction of many resonant parameters for ^{24}Mg states. The $^{20}Ne(\alpha,^{12}C)^{12}C$ cross sections varied in magnitude from 3 μb/sr to 8.8 mb/sr. Simultaneously recorded were excitation functions for elastic and inelastic alpha scattering from ^{20}Ne to several final states in ^{20}Ne. The alpha scattering data involved another approximately 10 000 cross section measurements.

II. EXPERIMENTAL PROCEDURE

Up to 15 thin totally depleted surface barrier detectors measured the angular distributions of ^{12}C ions coming from the symmetric fission of the ^{24}Mg compound nucleus after excitation through the ^{20}Ne + alpha channel. The detectors were usually chosen thick enough to stop the ^{12}C ions,

 ©1981 The American Physical Society

but thin enough to allow alpha particles of the same energy to deposit only a part of their energy. However, one or two detectors stopped all the alpha particles. The target consisted of differentially pumped natural neon gas (90.92% ^{20}Ne). To reduce neon consumption helium gas was introduced as a buffer at the aperture of the first stage of differential pumping. The gas target pressure was monitored by a precision Bourdon gauge and any back diffusing helium was monitored by $\alpha + {}^4$He scattering in the alpha spectra. The cross sections were corrected for any helium partial pressure buildup. Beam heating of the target gas along the beam axis was insignificant. The target length was determined for each detector by a pair of slits whose acceptance had been precisely measured. The target was bombarded by the He^{++} beam from our pelletron-charged EN tandem Van de Graaff. The beam exited the chamber through a foil into a vacuum region where it entered an electrostatically suppressed Faraday cup. The spectrum for each detector was processed in our DDP-124 computer and then written on magnetic tape for later analysis.

Figure 1 shows sample spectra. The ^{12}C peaks are well isolated from the punch through alphas, and except at very forward angles there is almost no background.

Uncertainties that arise from random errors other than statistical and background subtraction errors are typically 3—5 % (greater at more forward angles). Statistical errors vary from 1—30 % and are shown on all figures if they exceed the size of the data points. Systematic errors for the whole range of the data varied from 2—3 % (again greater at more forward angles) and are discussed in detail in Ref. 24. The calibration using several (p,n), (d,n), and (α,n) threshold reaction energies determined the absolute energy to ± 6 keV. Billen[25] reported the reproducibility of sharp resonances as ± 3 keV. The energy resolution of the present experiment was at worst ± 4 keV and arose mainly from straggling of the beam in the target gas.[24]

III. RESULTS

Figures 2—4 show differential cross sections[44] for the ^{20}Ne$(\alpha,{}^{12}$C$)^{12}$C reaction. The lower energy scale in all figures is the laboratory energy of the alphas at the center of the target chamber. The upper energy scale is the corresponding excitation energy in ^{24}Mg. (Q=9.3125 MeV for the ^{20}Ne + alpha channel.) The excitation functions are for the laboratory angles from 10° to 85° in 5°

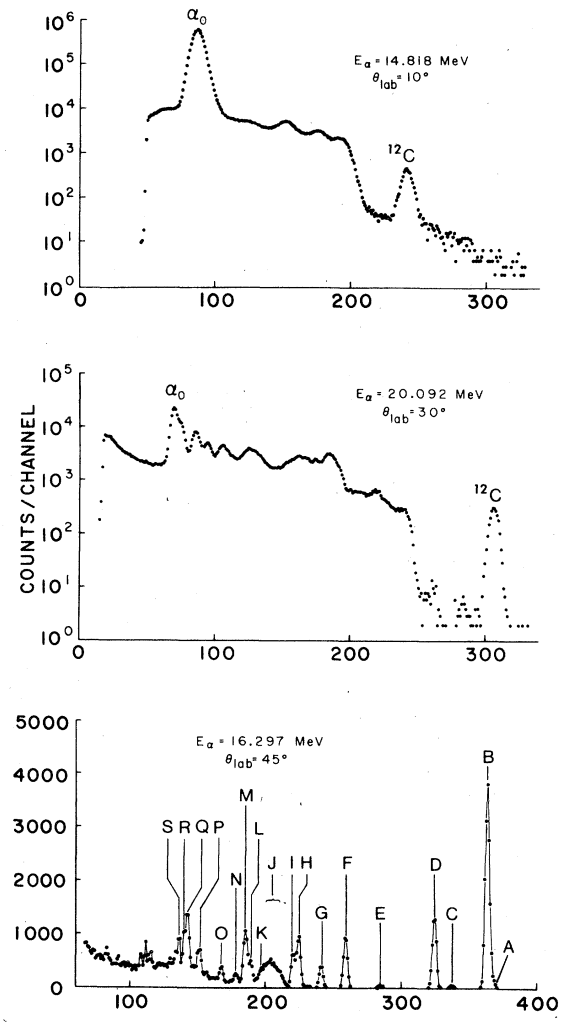

FIG. 1. Sample spectra from ^{20}Ne+α. The top two are from thin enough surface barrier detectors that the elastically scattered alphas, α_0, "punch through" (i.e., lose only part of their energy in the detector) and hence display considerable energy straggling. Note that for the ^{12}C peak significant background occurs only in the θ_{lab}=10° spectrum and that otherwise the ^{12}C peak stands out quite sharply. The lower spectrum is from a detector thick enough to stop all alpha particles. The elastic (designated *B*) and inelastic (*D*, 1.634 MeV; *F*, 4.248; *G*, 4.970; *H*, 5.621; *I*, 5.784; *K*, 6.724; *L*, 7.004; *M*, 7.168 and 7.191; *N*, 7.421; *O*, 7.829; *P*, 8.449; *Q*, 8.694; *R*, 8.777; and *S*, 8.848) groups are quite distinct for levels up to 8.85 MeV in excitation in ^{20}Ne. Groups from ^{22}Ne$(\alpha,\alpha)^{22}$Ne (8.82% of natural neon) also appear (*A*, ground state; *C*, 1.275 MeV; and *E*, 3.357). The broad peak around channel 205 (*J*) arises from the ^{4}He$(\alpha,\alpha)^4$He scattering (some of the buffer gas back diffuses into the chamber). This yield permits a correction for the average amount of helium contamination of the neon target gas.

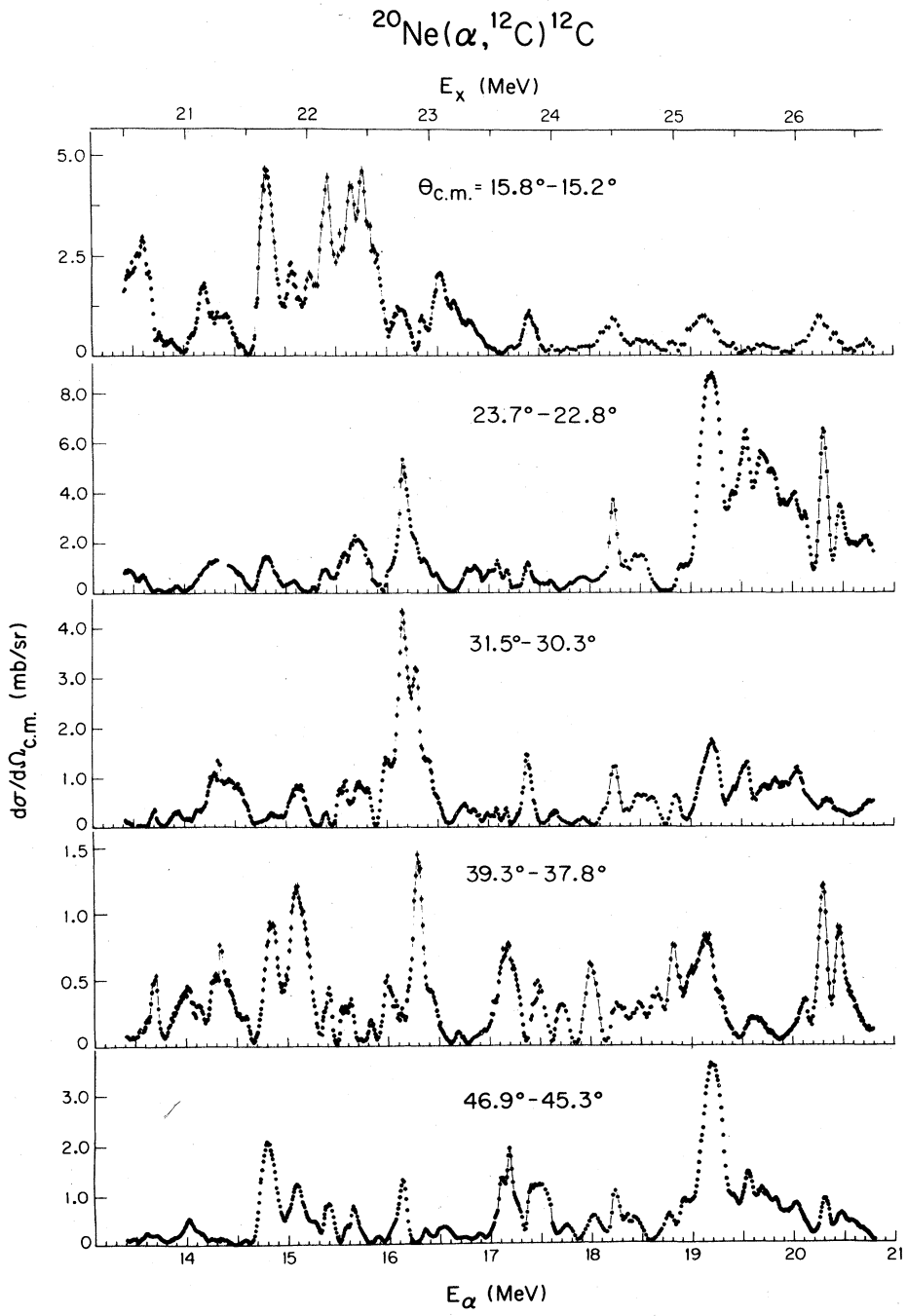

FIG. 2. Cross sections at forward laboratory angles. Error bars include counting statistics and background subtraction. They appear only if larger than the point size. The angles indicated correspond to center of mass angles at the ends of the energy range.

increments and are arranged progressively in that order. The center of mass angles depend on the bombarding energy, and their variation from lowest to highest alpha energy is indicated on each excitation function. Gaps in some of the excitation functions occurred when a detector malfunctioned during a run.

As mentioned previously, in 1963 Lassen and Olsen[4] measured an excitation function at 90° in the center of mass angle. Comparison with the

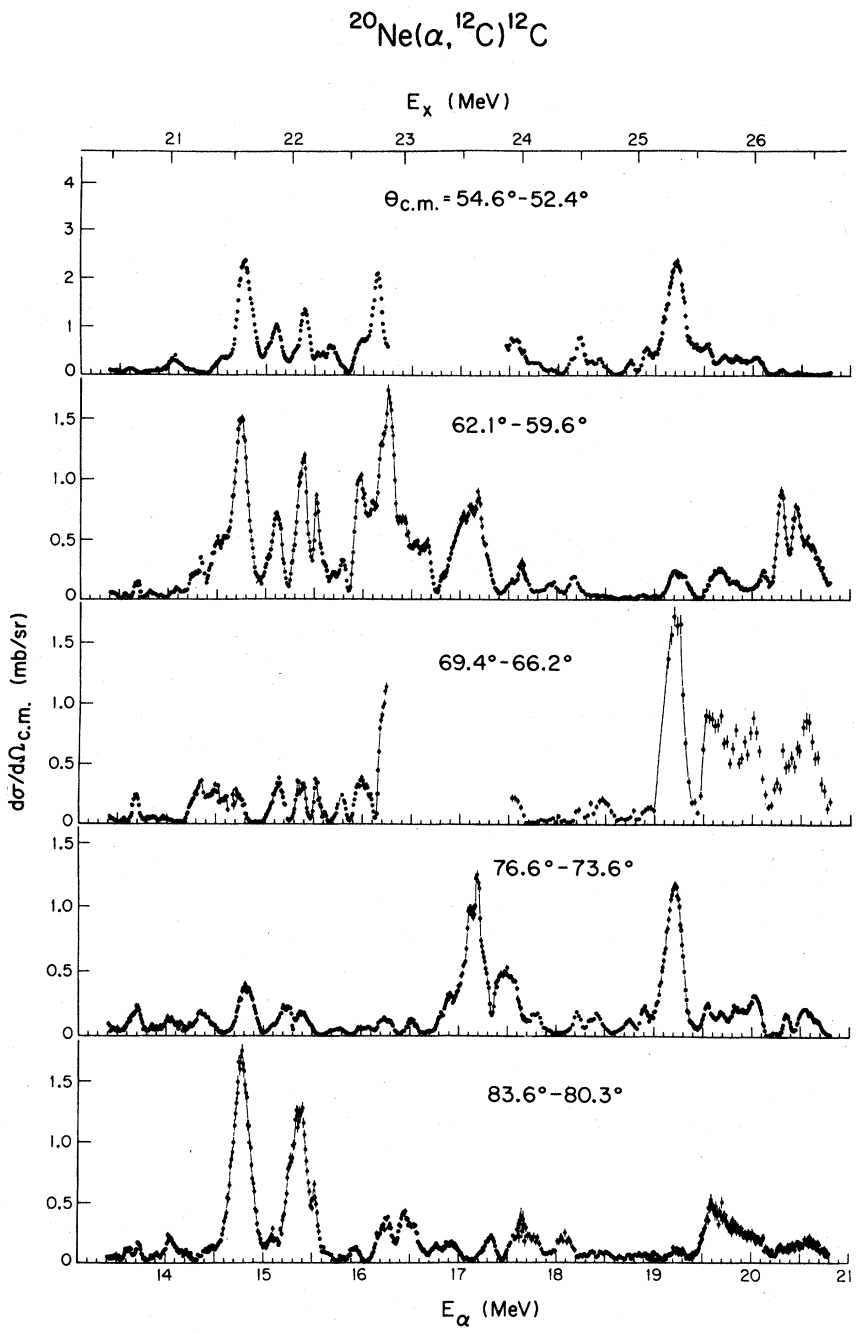

FIG. 3. Same as Fig. 2 except at intermediate angles.

$\theta_{c.m.} = 90° - 86.9°$ excitation function in Fig. 4 indicates that their cross sections exceed the present data by about a factor of 3. The broad structures of both data sets agree nicely. The results of Kuehner *et al.*,[6] also in 1963, when adjusted for the different phase space in the inverse reaction, agree with Lassen and Olsen, but are not an independent normalization. The recent results of Voit *et al.*[13] lie about 40% higher than those of this experiment (see Fig. 6). Erb *et al.*[10] originally normalized their data to that of Kuehner *et al.*, but recently[26] renormalized it to agree with the work of Voit *et al.*

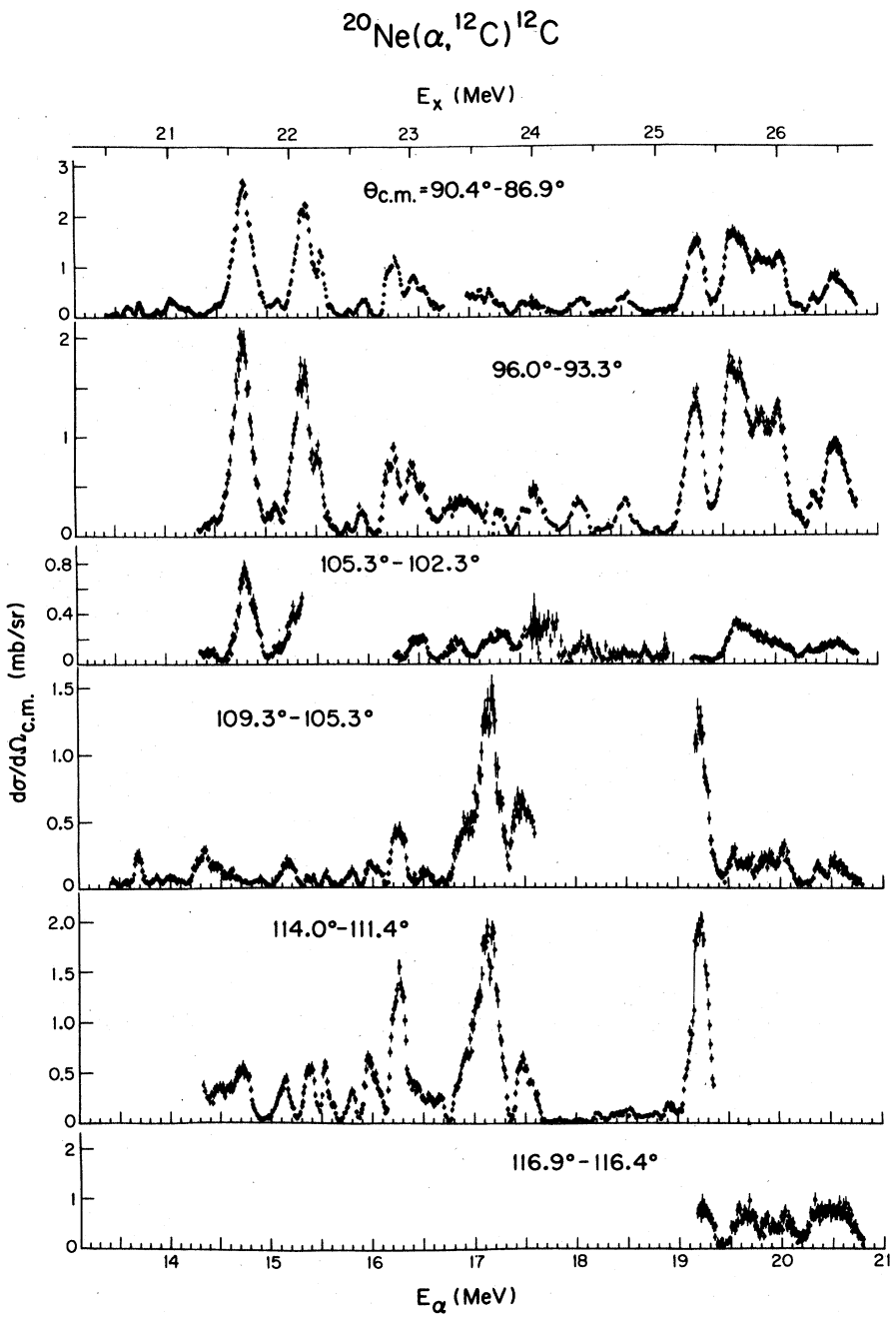

FIG. 4. Same as Fig. 2 except at back angles.

Thus, there appear to be only two independent cross section determinations previous to the present data. Lassen and Olsen[4] integrated their beam current by passing the beam through a tantalum foil window at the end of the target and into an apparently unsuppressed Faraday cup which was evacuated by means of a rubber tube connected to the cyclotron vacuum. If the Faraday cup was also collecting electrons knocked forward by the beam as it was passing through the neon gas and the window, then the apparent integrated beam charge would have been reduced, and consequently the apparent

cross section would be higher. The remaining measurements were made with a carbon beam incident on a solid carbon target. Solid carbon targets are susceptible to carbon buildup with time and heavy ion beams are plagued by charge state uncertainties. Voit *et al.*[27] reported that normalization of their data depended on a Faraday cup and use of monitor counters to monitor carbon buildup, but they have no explanation for the discrepancy. As mentioned previously, the systematic errors in the absolute cross sections amounted to only 2–3 %.

The data were expanded in terms of Legendre polynomials

$$\left.\frac{d\sigma}{d\Omega}\right|_{\text{c.m.}} = \sum_{\nu=0}^{\nu_{\max}} a_\nu P_\nu(\cos\theta) , \qquad (1)$$

where ν takes on only even values because the final channel in this reaction consists of two identical particles, and hence, the center of mass angular distributions must be symmetric about 90°. Since all particles involved in the reaction are 0^+, only natural parity states are observable; and because of the identical particles, only even spin positive parity states are possible. The Legendre expansion for each angular distribution and for several different maximum orders $\nu_{\max}$ were calculated. The best fit was chosen for the $\nu_{\max}$ such that the chi squared per degree of freedom (χ^2/N) reached a reasonable value and did not improve for higher $\nu_{\max}$. Since all of the particles are of zero spin, then any resonance of spin J will only contribute to a_ν up to $\nu=2J$. Thus the $\nu_{\max}$ for any region should give the maximum J of the resonances in that region. However, in some cases $\nu_{\max}$ was twice an odd number. This case occurs when strong resonances of spin J interfere with an otherwise insignificant structure in $\nu=2(J+2)$ to give an appreciable interference term at $\nu=2J+2$. Figure 5 shows samples of angular distributions and Legendre expansions to the data. Clearly the data are symmetric about 90°. In some cases, such as that at $E_\alpha=14.808$ MeV, one can easily guess the spin of the structure ($J=4$) by examination of the angular distribution. However, one should beware of such facile techniques when it is known that the density of resonances is large, as is the case here.

The results of the Legendre fitting are presented in Figs. 6 and 7. That the a_ν are negative in some regions is proof that there are not resonances of a single J only in those regions. That certain regions of a_ν (for example, above $E_\alpha=19$ MeV) change sign and magnitude in a consistent fashion means that the resonances of different J are not randomly

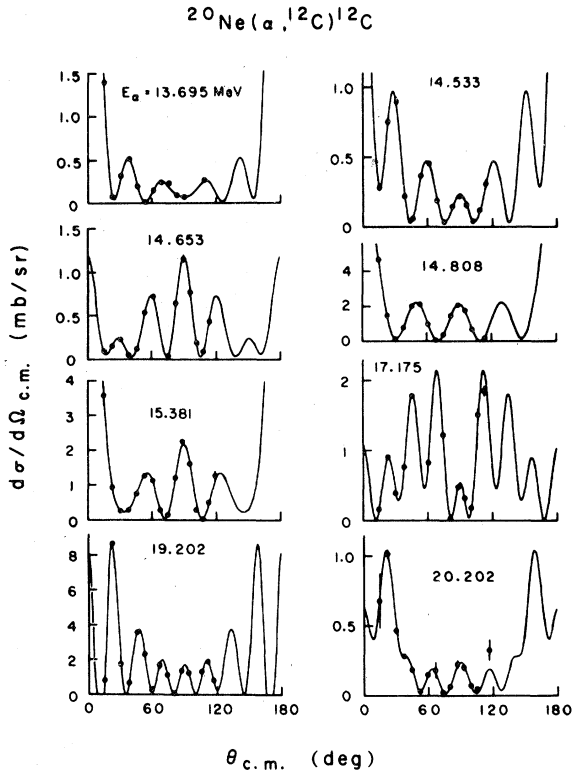

FIG. 5. Sample angular distributions at selected energies. Error bars appear only when they exceed the point size. The solid line represents the Legendre polynomial fit in each case. Notice that the angular distributions are all symmetric about 90° in the center of mass.

scattered throughout the region, but that the spins of the strong resonances are pretty much the same in the region.

Of interest is the lowest energy at which a given a_ν is necessary. In Fig. 7, a_{20} ($J=10$) makes no contribution below $E_x=25$ MeV, a_{16} ($J=8$) is very close to zero below $E_x=22.7$ MeV, and a_{12} ($J=6$) is also near zero although it is still making some contribution at $E_x=20.5$ MeV, the lowest energy of this work. Almqvist *et al.*,[5] from the inverse reaction $^{12}C(^{12}C,\alpha)^{20}Ne$, and at energies about 400 keV below the lowest energy reported here, confirm that no a_{12} term is necessary and, therefore, that $J=6$ is not making a contribution at these energies ($E_x<20$ MeV). Their data also indicate that the a_8 term ($J=4$) is becoming weak, although it is still measurable at their lowest energy of $E_x=19.3$ MeV. These cutoffs probably lie several MeV above the centrifugal-Coulomb barrier energy in the ^{20}Ne + alpha entrance channel for

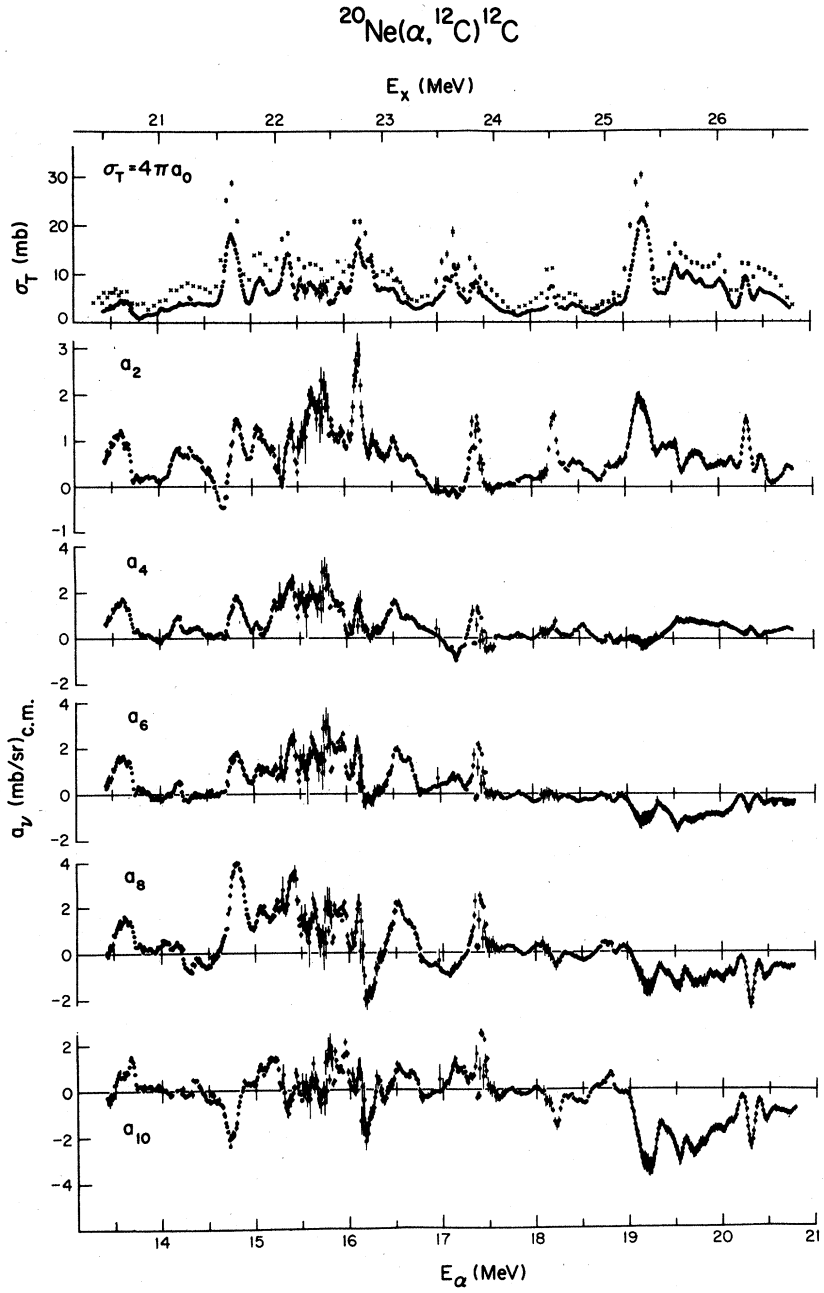

FIG. 6. The Legendre polynomial expansion coefficients $a_0 - a_{10}$. The total cross section $4\pi a_0$ is in the top frame. The widely spaced $\times$'s in this frame correspond to the total cross sections of Voit *et al.* (Ref. 13) for the inverse reaction $^{12}C(^{12}C,\alpha)^{20}Ne$ as calculated by detailed balance. The cross sections of Voit *et al.* cross sections are larger by about 40%.

each J. In the reaction $^{20}Ne(\alpha,\alpha_0)^{20}Ne$ at lower energies, a spin as high as $J=7$ was observed as low as $E_x=16.5$ MeV ($E_\alpha=8.5$ MeV), and $J=6$ was observed as low as $E_x=14.7$ MeV ($E_\alpha=6.5$ MeV).[28] Thus the threshold energy for higher J strength does not involve simple centrifugal-Coulomb barrier inhibition in the ^{20}Ne + alpha entrance channel.

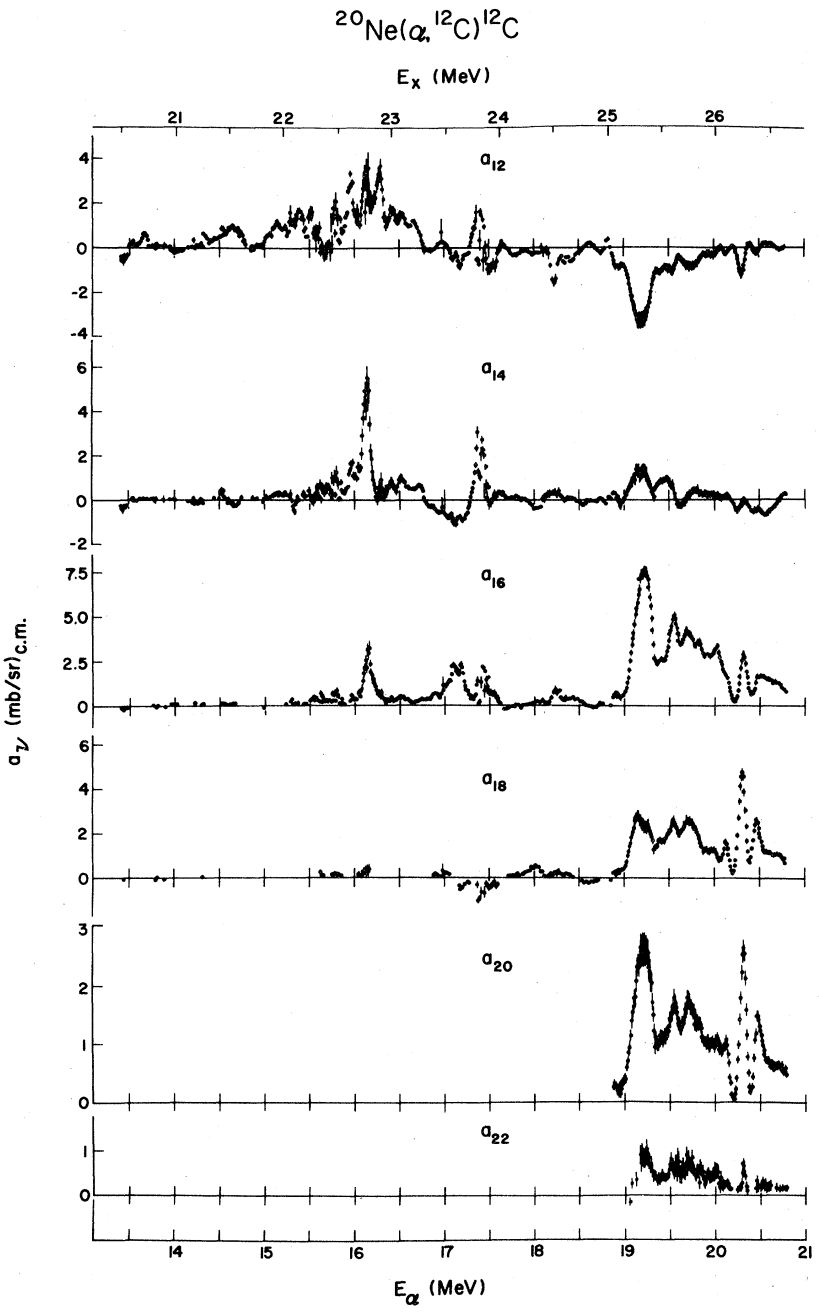

FIG. 7. The Legendre polynomial expansion coefficients $a_{12}-a_{22}$. See also Fig. 6.

Figures 8 and 9 contain the excitation functions[44] for elastically and inelastically scattered alpha particles that were measured simultaneously with the ^{20}Ne(α,^{12}C)^{12}C data at one or two angles. Also included in the center of Fig. 8 is the total cross section for the ^{20}Ne(α,^{12}C)^{12}C reaction. In general, while there are not dramatic correlations between the alpha decay channels and the ^{12}C + ^{12}C fission channel, some of the strong states seen in the total cross section for ^{20}Ne(α,^{12}C)^{12}C may correspond to structure in some of the alpha channels (for example, at $E_\alpha = 19.2$ MeV). At low

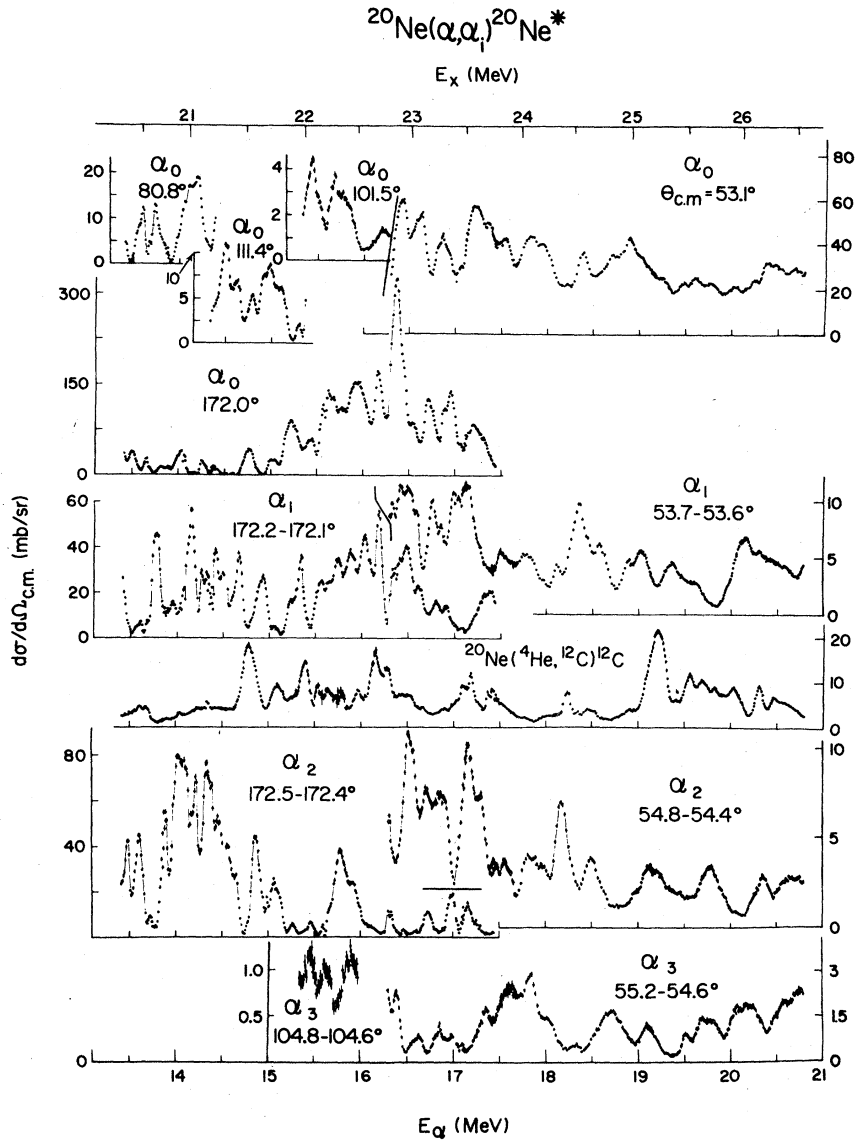

FIG. 8. Yields of elastically scattered alphas (α_0) and inelastically scattered alphas from the first excited (α_1, 2^+, 1.634 MeV), second excited (α_2, 4^+, 4.248 MeV) and third excited (α_3, 2^-, 4.970 MeV) states of ^{20}Ne and for comparison the total cross section for the $^{20}Ne(\alpha,^{12}C)^{12}C$ reaction (from Fig. 6).

energies, the structure in the elastic and inelastic alpha channels is quite marked and of the order of 50—100 keV wide. Moving to higher energies the structure broadens and becomes much more overlapping. These excitation functions in ^{20}Ne + alpha elastic and inelastic scattering are the first such data in this region.

IV. ANALYSIS

The most complete description of any reaction involves determination of the S matrix and then derivation of resonant parameters from the observed energy dependence of the various S-matrix elements. However, at energies of this work the reaction in question should involve partial waves up to $L=10$. Since the outgoing channel consists of two identical particles, we need only consider even L's, and hence, six complex S-matrix elements. An overall phase factor is arbitrary, so 11 parameters should fit any angular distribution. However, up to 32 independent solutions exist for such a fit. The possibility of picking the correct physical solution at any one energy and following

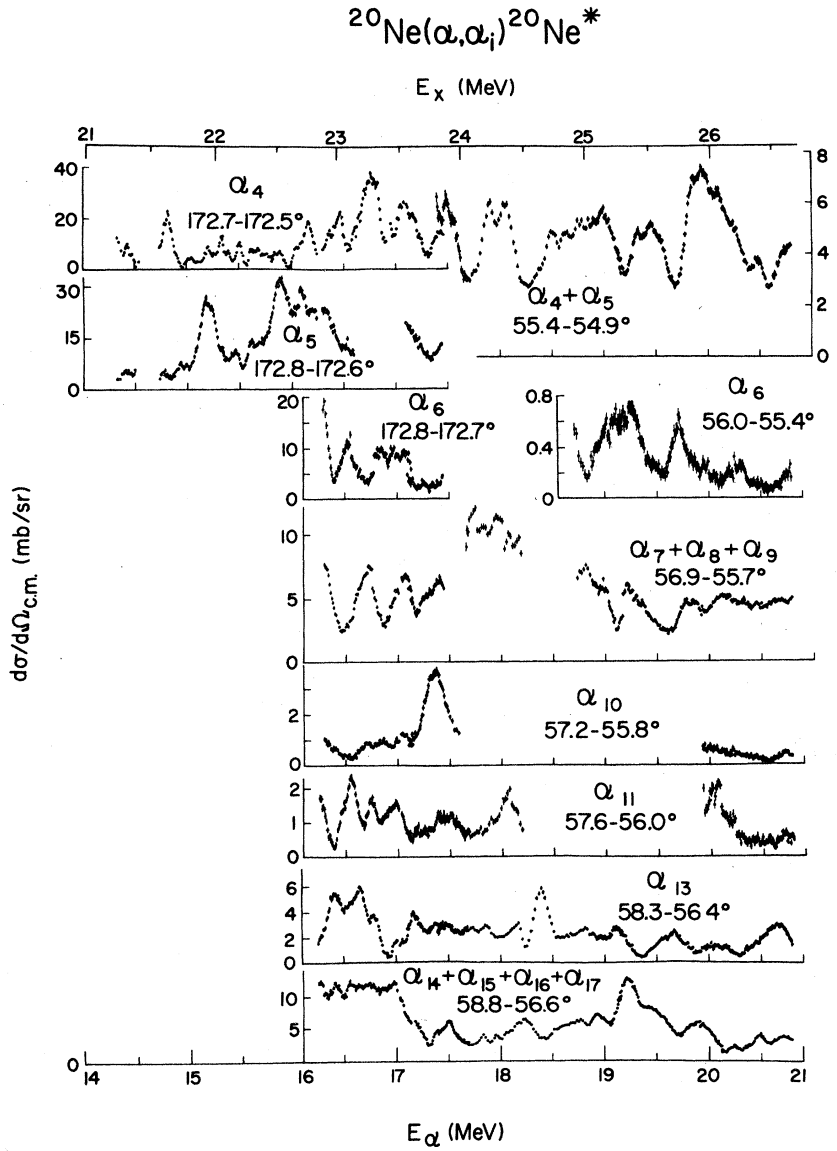

FIG. 9. Like Fig. 8 except for yields of α_i from higher excited states of ^{20}Ne: α_4, 3^-, 5.621 MeV; α_5, 1^-, 5.784 MeV; α_6, 0^+, 6.724 MeV; ($\alpha_7-\alpha_9$), (4^-, 3^-,0^+), (7.00—7.19 MeV); α_{10}, 2^+, 7.421 MeV; α_{11}, 2^+, 7.829 MeV; α_{13}, 5^-, 8.449 MeV; ($\alpha_{14}-\alpha_{17}$), (1^-, 6^+, 2^+, 1^-), (8.694—8.848 MeV).

that solution from energy to energy is, therefore, almost hopeless. Instead, we separate the reaction into a nonresonant and a resonant amplitude and make use of both the energy and angle dependence of the cross section to identify the partial waves. We let the nonresonant amplitude $\rho(\theta,E)$ vary linearly with energy in the approach used so successfully by Häusser *et al.*[29] and by Billen.[25] The resonances are expressed in the standard Breit-Wigner form, and the phase difference $\phi_l(\theta,E)$ between each resonance and the nonresonant background can vary linearly with energy:

$$\frac{d\sigma}{d\Omega}(\theta,E)=\left|\rho(\theta,E)\exp[i\chi(\theta)]+\frac{i}{2k}\sum_{l=l_r}(2l+1)\frac{\Gamma_i}{\Gamma}[\exp(2i\beta_l)-1]\exp[2i\phi_l(\theta,E)]P_l(\cos\theta)\right|^2, \quad (2)$$

where $\chi(\theta)$ is the phase of the nonresonant term, which in actual computation is set equal to zero as there is one overall phase that can be ignored, and where the sum is over resonances in the fitting region. The resonant phase shift is given by

$$\beta_l = \tan^{-1}\left[\frac{\Gamma/2}{E_r - E}\right]. \quad (3)$$

The parameters $\rho(\theta,E)$ and $\phi_l(\theta,E)$ were adjusted separately at each angle θ, but the resonant parameters E_r, Γ and the width $\Gamma_i = (\Gamma_\alpha \Gamma_c)^{1/2}$ were the same for all angles and energies of the fitting region. More detailed discussions of the resonant fitting procedure are in Refs. 24 and 25.

Equation (2) has been used successfully to parametrize the data over most of the energy regions. The results are summarized in Table I. A discussion of the derivation of the uncertainties in the resonant parameters reported in Table I may be found in Ref. 25.

The data are very complicated and contain numerous overlapping levels. Where some resonances are much stronger than adjacent weaker resonances, I could not extract parameters for those weak resonances (this would be a problem for any fitting technique). Consequently, there may be an insufficient number of resonances assumed in any given region to give a good chi square per degree of freedom (χ^2/N). I based judgments as to the quality of a fit on the values of χ^2/N and actual inspection of the fits and final parameters.

There are some problems associated with the specific fitting technique. First, poor fits can arise from assuming the wrong J for a resonance or from bad initial guesses for the resonant parameters. The program then often excessively broadens the Γ while trying to fit the data by oscillations in the cross term between the background and the assumed resonance terms. To do this it changes the phase $\phi_l(\theta,E)$ as a function of energy in an extreme manner (one or more oscillations over the width of the resonance). Examination of the output $\phi_l(\theta,E)$ will reveal this problem. Moreover, an improper resonance shape results, as well as a poorer χ^2/N. Second, the fitted region should extend far enough beyond the fitted resonances to well determine the nonresonant term. This was often not possible with our limited computer capacity. As a result, levels near the edge of a fitting region have more uncertainty in the resonant parameters, especially if they have appreciable width. I cannot distinguish between the permitted linear background and resonances that are much broader than about half the width of the fitting region (which is usually less than 600 keV). The program can fit a maximum of six resonances at a time. Häusser *et al.*[29] also had trouble fitting broad resonances.

V. DISCUSSION OF FITS AND IMPLIED ^{24}Mg STATES

A. Energy region from $E_x = 20.56$ to 20.80 MeV

Figures 2–4 show that most of the structure vanishes at $\theta_{c.m.} = 31°$, 69°, and 109°. Since $P_4(\cos\theta) \approx 0$ for these angles, this region is dominated by one or more 4^+ resonances. However, at these P_4 zeros an additional resonance appears at $E_x = 20.729$ MeV which is probably 2^+ since it vanishes at $\theta_{c.m.} = 54.6°$ where $P_2 \approx 0$. The structure in a_{12} in Fig. 7 indicates that some $L = 6$ strength is also present. Using the $J = 2$ resonance above and only one $J = 4$ at $E_x = 20.678$ MeV resulted in a fit of χ^2/N of 2.11. Including additional $J = 4$ or $J = 6$ resonances did not improve the fit. Others[13,14,30–33] have reported 2^+ and 4^+ resonances in this region via other decay channels. Except for a 4^+ resonance[30,33] which has $E_x = 20.76$ MeV and $\Gamma = 125$ keV, they probably do not correspond to resonances reported here, since the E_x differ by > 120 keV. It is interesting to observe that all resonances seen by Voit *et al.*[13] in the ^{12}C(^{12}C,α_6)^{20}Ne* reaction have energies from 0.19 to 0.27 MeV (increasing with E) above the positions of resonances of identical spin seen by them in the ^{12}C(^{12}C,α_0)^{20}Ne reaction. The 0.12 MeV separation between their 4^+ resonance at $E_x = 20.80$ MeV and the present 4^+ resonance at $E_x = 20.678$ MeV fits this pattern. For a detailed discussion see Ref. 24.

B. Energy region from $E_x = 20.80$ to 21.22 MeV

I failed to achieve any fits with $\chi^2/N < 2.5$ in this region. The lack of a decent fit suggests that there are more overlapping weak resonances than the program can handle, but not a large enough number to treat as background. Inspection of the total cross section (Fig. 6) shows one weak resonance at $E_x \approx 20.99$ MeV with a width $\Gamma \approx 70$ keV. Although several authors[31,33,34] report unassigned resonances in this region, only Erb *et al.*[33] list one at $E_x = 20.98$ MeV with $\Gamma > 75$ keV which could correspond to the one I observed at $E_x = 20.99$ MeV.

TABLE I. ^{24}Mg levels observed via ^{20}Ne(α, ^{12}C)^{12}C. Except for E_α, all energies are in the center of mass system.

E_α (lab) (MeV±keV)	E_x[a] (^{24}Mg) (MeV±keV)	Γ (keV)	Present work $\frac{(\Gamma_\alpha\Gamma_c)^{1/2}}{\Gamma}$ in percent	J^π	$\Gamma_c >$[b]	E_x (MeV)	J^π	Previous work[c] Γ (keV)	Γ_c (keV)	Ref.
13.644± 5	20.678± 6	100±10	13.0±0.6	4^+	1.7	20.77		125	14±4	33
13.706± 4	20.729± 5	58± 9	9.3±0.9	2^+						
(unfitted between E_x=20.8−21.22 MeV)										
~14.02	~20.99	~70				20.98		>75		33
(14.33)	(21.25)	(300)		(2^+)		21.18				34
						21.23		~75		33
14.360± 6	21.274± 6	43±14	6.5±1.3	0^+		21.38		~75		33
						21.33				34
14.657±29	21.521±24	172±60	3.2±0.6	6^+		21.43	6^+	180		11
						21.51		110	>9	33
						21.53				34
(14.78)	(21.625)	(200)	(2)	(4^+)						
14.787± 8	21.630± 8	174±13	17.7±0.7	4^+	5.3	21.64	4^+			13
						21.64	4^+	145	>4.5	10
						21.7				34
						21.64		125	>22	33
15.010± 5	21.815± 6	70±10	6.8±0.5	6^+		21.83				34
						21.78				33
15.107± 5	21.896± 5	130±11	10.9±0.4	6^+	1.5					
15.256±10	22.020± 9	61±20	3.6±0.9	4^+		21.98	(4^+)			14
~15.34	~22.09	~30	~2	(6^+)						
15.409± 6	22.147± 6	68±10	6.5±0.5	6^+		22.19	4^+			13
						22.20				34
						22.18		175	>39	33
15.523± 6	22.243± 6	52±11	4.2±0.5	6^+						
15.583± 4	22.292± 5	41± 7	5.4±0.6	6^+						
(15.60)	(22.31)	(250)	(4)	(4^+)						
15.629± 6	22.330± 6	54±11	5.6±0.8	4^+						
(15.72)	(22.41)	(100)	(4)	(6^+)		22.36	6^+			9,11
						22.38				34
						22.36				33
15.877± 6	22.537± 6	110±16	6.8±0.5	6^+						
15.980± 4	22.623± 5	44± 8	4.8±0.5	4^+						
16.146± 6	22.761± 6	88±11	6.3±0.5	8^+		22.8	8^+			9,11
16.167± 9	22.779± 8	49±17	3.7±0.8	6^+		22.79	6^+			13
						22.78	6^+	~200[d]		39

TABLE I. *(Continued).*

E_α (lab) (MeV±keV)	E_x[a] (^{24}Mg) (MeV±keV)	Present work Γ (keV)	Present work $\frac{(\Gamma_\alpha\Gamma_c)^{1/2}}{\Gamma}$ in percent	J^π	$\Gamma_c >$[b]	Previous work[c] E_x (MeV)	J^π	Γ (keV)	Γ_c (keV)	Ref.
						22.78	6^+			14
						22.8				34
						22.76		~125	>8.5	33
16.258± 8	22.854± 8	~25	~1.5	6^+						
16.284± 6	22.876± 6	76±10	6.8±0.6	6^+						
16.338± 7	22.921± 7	53±13	3.3±0.5	4^+						
16.446±10	23.011± 9	59±20	2.7±0.5	4^+		23.03				34
						(23.05)				33
~16.56	~23.11	~50	~2	(4^+)						
16.712± 9	23.233± 8	120±21	9.2±0.7	6^+	1	23.26		~125		33
(16.82)	(23.32)	(80)	(5)	(0^+)						
16.932±13	23.416±11	104±18	6.5±0.5	8^+						
17.087± 5	23.545± 6	30± 8	3.6±0.7	8^+		(23.53)		>75		33
17.154±16	23.601±14	188±58	3.7±0.6	6^+						
17.181± 4	23.623± 5	36± 7	6.4±0.6	8^+		23.58	8^+			34
						23.60		100		33
17.349± 7	23.763± 7	68±16	4.1±0.6	8^+		23.77	8^+	125		10
						23.77	8^+			13
						23.78				34
						23.78		100	7.5	33
(17.37)	(23.78)	(25)	(1)	(8^+)						
17.416±16	23.819±14	135±34	4.0±0.5	6^+						
(unfitted between E_x=23.97−24.35 MeV)										
~18.16	~24.44	~140	~3.5	(6^+)						
18.222± 5	24.490± 5	80± 7	9.7±0.5	8^+	0.8	24.53	8^+			6
						24.52	8^+			10
						24.56	8^+			13
18.363± 5	24.607± 6	40±10	5.0±1.1	4^+						
18.419± 9	24.653± 8	128±16	7.4±0.4	8^+		24.68	(8)			6
18.556± 7	24.768± 7	61±13	3.7±0.4	8^+						
18.814±21	24.983±17	89±32	4.2±1.0	6^+						
18.865±14	25.025±13	72±28	3.2±0.9	8^+		25.13	8^+			14
19.128±26	25.244±22	150±50	3.1±0.7	10^+						
19.229±11	25.328±10	202±16	14.2±0.6	8^+	4	25.2	8^+	145		4
						25.33				15
						25.3	8^+	200		6
						25.31	8^+			13
						25.1	8^+	~300[a]		39

TABLE I. *(Continued).*

E_α (lab) (MeV±keV)	E_x[a] (^{24}Mg) (MeV±keV)	Present work Γ (keV)	Present work $\frac{(\Gamma_\alpha\Gamma_c)^{1/2}}{\Gamma}$ in percent	J^π	$\Gamma_c >$[b]	E_x (MeV)	Previous work[c] J^π	Γ (keV)	Γ_c (keV)	Ref.
19.295±17	25.383±14	73±40	2.4±0.8	6^+						
19.511± 8	25.563± 8	103±18	5.7±0.7	6^+						
19.578± 5	25.619± 5	89±10	8.3±0.9	8^+						
(19.728±19)	(25.744±16)	(100)		$(8^+,10^+)$						
19.816±30	25.817±25	~50	~1.5	8^+						
20.041±11	26.005±10	81±17	3.7±0.4	8^+						
20.135± 9	26.083± 9	65±23	2.4±0.5	10^+						
20.312± 6	26.230± 6	85±10	7.4±0.6	10^+						
20.323±14	26.239±12	106±24	4.5±0.6	8^+						
20.457±10	26.351± 9	118±18	6.3±0.5	10^+		~26.3	(10)			6

[a]Includes random error of ±3.6 keV added in quadrature to uncertainty.
[b]Lower bound for ^{12}C partial width.
[c]^{20}Ne(α, ^{12}C)^{12}C and inverse reaction. However Refs. 40 and 41 include results of other ^{24}Mg exit channels.
[d]Large uncertainty in the experimental width.

C. Energy region from $E_x = 21.22$ to 21.40 MeV

Figure 10 shows a very narrow resonance at $E_x = 21.274$ MeV with $\Gamma = 43 \pm 14$ keV and a $J^\pi = 0^+$ fit which gave $\chi^2/N = 1.22$. Attempts to fit this resonance with other J's led to a χ^2/N of 1.53 at best (for a 6^+), and broadened the width by 30–40% (see the above discussion of problems with the fitting routine). Included in Fig. 10 are a few fits for other J's near $P_L \approx 0$. Although the differences between these other fits and the data are small, the fact that there are 100 degrees of freedom in this fit makes the difference between the chi squares significant. The region immediately above this resonance shows a broad 6^+ resonance at $E_x = 21.521$ MeV (see the following section). Inclusion of this resonance in the background of the narrow 0^+ might explain the relative success of the $J = 6$ fit. Only a $J^\pi = 0^+$ is sufficient to explain the data. No one else has seen this narrow resonance unless the 75 keV width Erb *et al.*[33] report for a state at $E_x = 21.23$ MeV is a considerable overestimate.

Figures 2–4 and 10 show that the background in this region and the region immediately below it is very small (< 50 μb/sr) only near $\theta_{\text{c.m.}} = 54.2°$ and near $\theta_{\text{c.m.}} = 89.7°$. This last minimum arises from interference between different l's since no even l can have a zero at 90°. The excitation functions, especially at $\theta_{\text{c.m.}} = 23.7°$ (Fig. 2) and $\theta_{\text{c.m.}} = 109.3°$ (Fig. 4) reveal what appears to be a broad ($\Gamma \approx 300$ keV) resonance at $E_x \approx 21.25$ MeV. Since at $\theta_{\text{c.m.}} = 54.7°$, $P_2 = 0$ and since this is the only zero at this broad structure, I tentatively suggest a broad 2^+ resonance at this energy but have attempted no fits with such a resonance.

D. Energy region from $E_x = 21.39$ to 21.98 MeV

The Legendre polynomial coefficients in Fig. 6, the angular distribution at $E_\alpha = 14.808$ MeV in Fig. 5, and the fit shown in Fig. 11 all indicate that a 4^+ level at $E_x = 21.630$ MeV dominates this region. To obtain the χ^2/N of 1.65 fit shown in Fig. 11 required also including a 6^+ at $E_x = 21.521$ MeV and another weak 4^+ state at $E_x = 21.625$ MeV. Excluding the second 4^+ gave a $\chi^2/N > 2$. The second (weak) 4^+ does not appear as a separate peak but gives a slightly asymmetric shape to the resonant cross section which is dominated by the strong 4^+. Such an asymmetry might also arise from a rapid change in penetrability of an

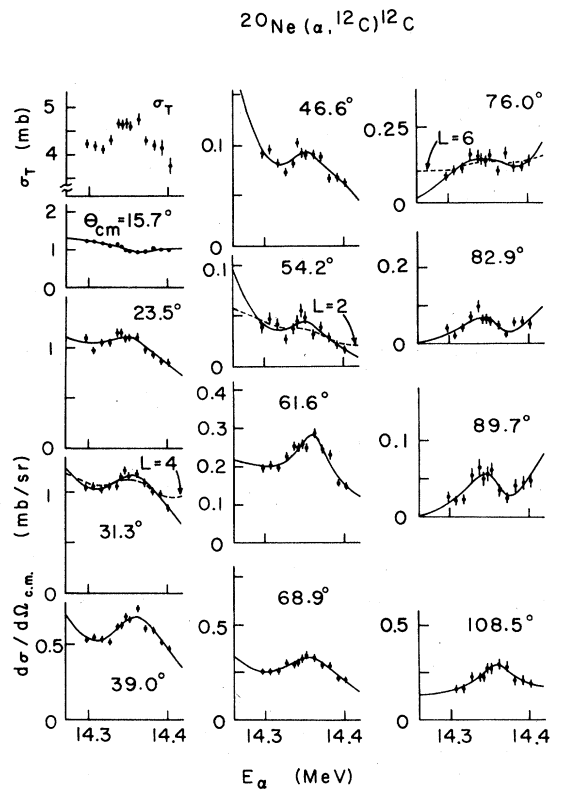

FIG. 10. Resonance at $E_x=21.27$ MeV. The solid curves show a $J^\pi=0^+$ fit with $\chi^2/N=1.22$. The dashed lines at some angles show fits with other L's near the corresponding zeros for P_L. The total cross section in this region is shown at the upper left (note the suppressed zero).

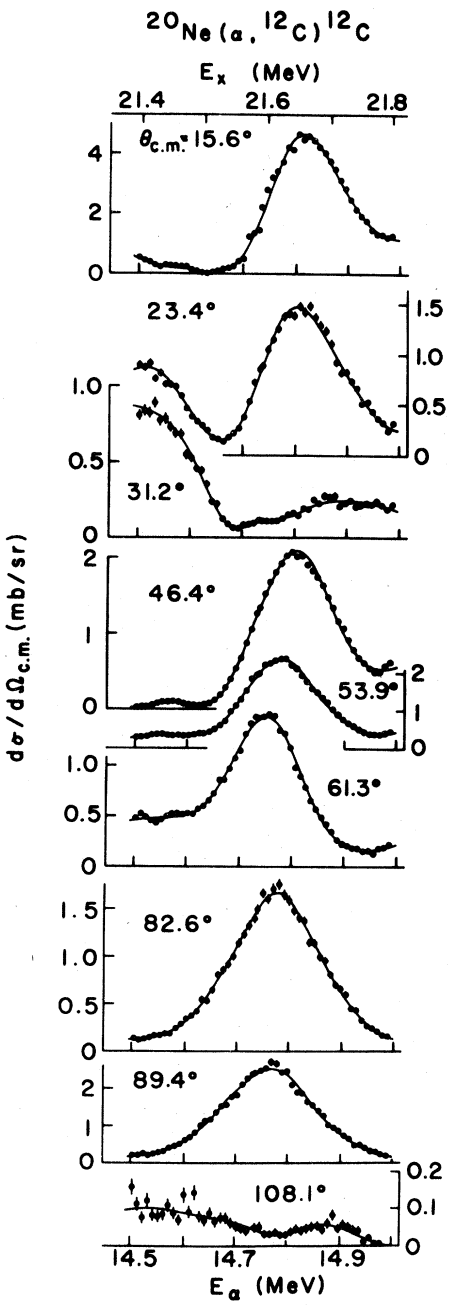

FIG. 11. Sample fits for $E_x=21.39$ to 21.80 MeV. A $\chi^2/N=1.65$ resulted from three resonances at $E_x=21.630$ MeV (4^+, 17.7%, 174 keV); $E_x=21.521$ MeV (6^+, 3.2%, 172 keV); and $E_x=(21.625)$ MeV [(4^+), (2%), (200) keV].

opening channel. In the present case two new proton channels open at $E_x=20.73$ MeV and $E_x=21.50$ MeV and these channels become strongly populated at higher excitation energies.[35,36] Therefore, I am not sure that a weak second 4^+ state exists, even though the χ^2/N improves considerably. Hence, in Table I, I list the second 4^+ in parenthesis. In Fig. 11, clearly the 4^+ is no longer present at $\theta_{\text{c.m.}}=31.2°$ [$P_4(30.60°)=0$], but there is still evidence of the 6^+ at $E_x=21.521$ MeV. At $\theta_{\text{c.m.}}=108.1°$ the cross section is very low, as we are near both a zero of P_4 (109.9°) and a zero of P_6 (103.8°). The strong 4^+ has been previously observed in several studies[10,13,33] and the resonant parameters are in reasonable agreement with the present ones if one changes the value of Erb *et al.*[10] of $\Gamma_\alpha\Gamma_c=1700$ (keV)^2 to $\Gamma_\alpha\Gamma_c=640$ (keV)^2 because of an overall normalization correction[26] to their data. Basrak *et al.*[11] report a 6^+ resonance at $E_x=21.43\pm0.05$ MeV based on the angular distribution of the ^{12}C(^{12}C,α_0)^{20}Ne reaction. They estimate $\Gamma=180$ keV and so almost agree with the 6^+ at $E_x=21.521\pm0.024$ MeV with $\Gamma=172\pm60$. Erb *et al.*[33] observed a resonance at $E_x=21.51$ MeV

$\Gamma=110$ keV, $\Gamma_c \geq 9$ keV, which they assumed to be 6^+.

To fit the region from $E_x=21.76$ to 21.98 MeV with $\chi^2/N=1.06$ required only two 6^+'s at $E_x=21.815$ and 21.896 MeV and the tail of the lower strong 4^+ ($E_x=21.630$ MeV). With only one 6^+ at $E_x=21.9$ MeV the χ^2/N increased to 1.72. Although several groups[13,33,34,37] report resonant structure in various channels for this excitation range, only two assignments have been made: (1) Voit *et al.*[13] claim a 4^+ at $E_x=21.83$ MeV via the $^{12}C(^{12}C,\alpha_6)^{20}Ne^*$ (0^+, 6.72 MeV) reaction, but if the assignment is correct, its absence in the present data implies a very small Γ_α; (2) Sandorfi and Nathan[37] report a broad ($\Gamma=261\pm74$ keV) 2^+ state, $E_x=21.98\pm0.03$ MeV in the $^{12}C(^{12}C,\gamma)^{24}Mg$ reaction with $(2J+1)\Gamma_\gamma\Gamma_c/\Gamma=1.37\pm0.27$ eV. However, this resonance is not seen by Kuhlmann *et al.*[38] in the $^{20}Ne(\alpha,\gamma)^{24}Mg$ reaction, a result consistent with a small Γ_{α_0}, and so we should not see it. Furthermore, a weak resonance of this width at the edge of the fitting region might be included in the linear background term.

E. Energy region from $E_x=21.93$ to 22.20 MeV

Figure 12 shows a $\chi^2/N=1.47$ fit achieved by using three resonances, a 4^+ at $E_x=22.020$ MeV, a 6^+ at $E_x\approx22.09$ MeV ($\Gamma\approx30$ keV), and a 6^+ at $E_x=22.147$ MeV, plus the tail of the 6^+ at $E_x=21.896$ MeV. Note that in Fig. 12 the 4^+ has vanished at $\theta_{c.m.}=31.0°$ [$P_4(30.6°)=0$] and $\theta_{c.m.}=68.3°$ [$P_4(70.1°=0$] and has almost vanished at $\theta_{c.m.}=107.7°$ and 113.4° [$P_4(109.9°=0$]. An angular distribution in the vicinity of the 6^+ (Fig. 5 at $E_\alpha=15.381$ MeV) indicates a strong $L=4$ and probably requires a strong $L=4$ resonance that is of a width comparable to or larger than the region of analysis, and hence, has been missed by being included in the background terms. Evidence for such a broad resonance also exists in the following section. If I include the possible broad 4^+ at $E_x=22.31$ MeV, the total χ^2 drops from 445.5 to 422.3, but the χ^2/N increases slightly to 1.56. This result indicates that the background was successfully mimicking the broad 4^+. Nonetheless, $L=6$ strength is required in the region, as can be seen by inspecting a_{12} of Fig. 7. I tried changing the strong 6^+ at $E_x=22.09$ MeV to a 4^+, but failed to achieve a decent fit. In Fig. 12 at $\theta_{c.m.}=31°$ and 68.3° the structure from the resonances at $E_x=22.09$ and 22.147 MeV is still present. Since

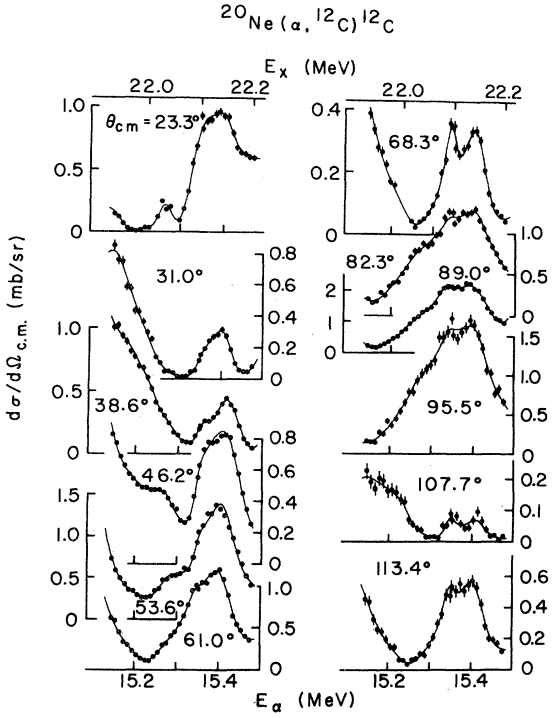

FIG. 12. Sample fits for $E_x=21.93-22.20$ MeV. A $\chi^2/N=1.47$ resulted from three resonances at $E_x=22.020$ MeV (4^+, 3.6%, 61 keV); $E_x\approx22.09$ MeV (6^+, ~2%, 30 keV); and $E_x=22.147$ MeV (6^+, 6.5%, 68 keV) plus the tail of the 6^+ at $E_x=21.896$ MeV.

these angles are near zeros of P_4, this structure is not $L=4$.

Coçu *et al.*[14] reported a possible 4^+ at $E_x=21.98$ MeV (Ref. 5) based on Legendre fitting of $^{12}C(^{12}C,\alpha_0)^{20}Ne$ angular distributions. Andritsopoulos *et al.*[34] found a resonance at $E_x=22.20$ MeV in the gamma decay from residual nuclei in several reactions from $^{12}C+^{12}C$. Erb *et al.*,[33] using the same reactions, observed a resonance at $E_x=22.18$ MeV ($\Gamma=175$ keV) which they assumed (from previous work above) was a 4^+. They then derived a value for the minimum of $\Gamma_c>39$ keV. All these $L=4$ assignments for a resonance around $E_x=22.19$ MeV are based only on a qualitative examination of the angular distribution, and while they may imply a strong broad 4^+, they do not necessarily mean that the narrower resonance structure is 4^+. The present quantitative decomposition of the angular distribution and excitation function definitely requires that the narrower structure around $E_x=22.15$ is 6^+, not 4^+. Thus assign-

ment of spin based only on the appearance of an angular distribution is a risky business where there are overlapping resonances of different L. If the structure observed by Erb *et al.*[33] is the same as the 6^+ resonance at $E_x=22.147$ MeV (the disagreement in width and energy could result from their failure to resolve the other 6^+), then the minimum value for the carbon partial width becomes $\Gamma_c > 24$ keV.

F. Energy region from $E_x=22.17$ to 22.46 MeV

To achieve a $\chi^2/N=1.52$, I used three new 6^+ resonances and two new 4^+ resonances (see Table I) but I regard the 6^+ at $E_x=22.41$ MeV and the broad 4^+ at $E_x=22.31$ MeV as uncertain because of the relatively small decrease ($<20\%$) in χ^2/N which they produced. However, qualitative support for the broad 4^+ occurs in Figs. 2 and 3: At $\theta_{c.m.}=23.7°$ where $P_6\approx 0$, there is a large broad structure (in addition to the narrow 4^+ at $E_x=22.330$ MeV) and both structures vanish at $\theta_{c.m.}=69.4°$ where $P_4\approx 0$. The possible 6^+ may correspond to the 6^+ reported by Basrak *et al.*[9,11] at $E_x=22.36$ MeV. Their assignment came from a Legendre expansion of the cross sections for ^{12}C(^{12}C,α)^{20}Ne. The dependence of χ^2/N on ν_{max} was as follows: $\nu_{max}=4$, $\chi^2=14$; $\nu_{max}=8$, $\chi^2=1.1$; $\nu_{max}=12$, $\chi^2=0.13$, and steadily from there on. The dramatic drop in χ^2 from 14 to 1.1 as ν_{max} changes from 4 to 8 also supports the need for considerable $L=4$ strength at this energy. Others[13,33,34] also report resonances in various channels at $E_x\approx 22.36$ MeV. Only Voit *et al.*[13] make an assignment: a 4^+ at $E_x=22.33$ MeV in the ^{12}C(^{12}C,α_6)^{20}Ne* (0^+; 6.72 MeV) reaction.

G. Energy region from $E_x=22.48$ to 22.66 MeV

In this region the best fit had a $\chi^2/N=1.83$ and involved a 6^+ at $E_x=22.537$ MeV, a 4^+ at $E_x=22.623$ MeV, and the tail of the 8^+ at $E_x=22.761$ MeV (see the next section). The 6^+ appears at $\theta_{c.m.}=31.5°$ in Fig. 2 as a strong interference dip (nearly going to zero) and in Fig. 3 at $\theta_{c.m.}=54.6°$ as a low energy shoulder on the 8^+. The sharper structure just below $E_\alpha=16$ MeV at $\theta_{c.m.}=23.7°$ in Fig. 2 (near a zero of the sixth order Legendre polynomial) corresponds to the 4^+ at $E_x=22.623$ MeV. No resonances have ever been reported in this region before.

H. Energy region from $E_x=22.64$ to 22.97 MeV

Figure 13 shows samples of a $\chi^2/N=1.35$ fit involving five resonances: an 8^+ at $E_x=22.761$ MeV, a 6^+ at $E_x=22.779$ MeV, a 6^+ at

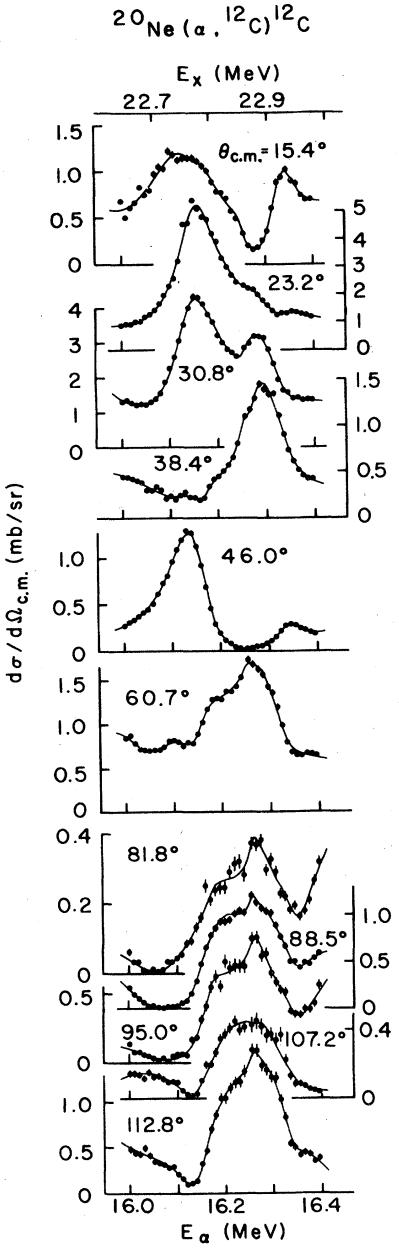

FIG. 13. Sample fits for $E_x=22.64$ to 22.97 MeV. A $\chi^2/N=1.35$ resulted from five resonances at $E_x=22.761$ MeV (8^+, 6.3%, 88 keV); $E_x=22.779$ MeV (6^+, 3.7%, 49 keV); $E_x=22.854$ MeV (6^+, ~1.5%, ~25 keV); $E_x=22.876$ MeV (6^+, 6.8%, 76 keV); and $E_x=22.921$ MeV (4^+, 3.3%, 53 keV).

$E_x = 22.854$ MeV, a 6^+ at $E_x = 22.876$ MeV, and a 4^+ at $E_x = 22.921$ MeV. Note that the 8^+ almost vanishes at 38.4° [$P_8(37.2°) = 0$] and is very small at 60.7° [$P_8(58.3°)$ and 81.8° $P_8(79.4°) = 0$]. The three 6^+'s nearly vanish at 23.2° [$P_6(21.2°) = 0$], 46.0° [$P_6(48.6°) = 0$], and 107.2° [$P_6(103.8°) = 0$]. Several groups[13,14,39] agree with the lower 6^+ assignment and Basrak *et al.*[11] support the 8^+ resonance at $E_x = 22.761$ MeV. Erb *et al.*[33] make no assignments, but by assuming that a resonance at $E_x = 22.76$ MeV, $\Gamma = 125$ keV is the 6^+ reported by others, they calculate $\Gamma_c \geq 8.5$ keV. The large width of Erb *et al.* as well as E_x suggest that a more likely identification would be with the 8^+ state reported here. If this is the case, $\Gamma = 88$ keV would permit $\Gamma_c \geq 4.5$ keV instead of their $\Gamma_c \geq 8.5$ keV.

I. Energy region from $E_x = 22.95$ to 23.16 MeV

A $\chi^2/N = 1.23$ fit required only a 4^+ at $E_x = 23.011$ MeV and a probable (4^+) at $E_x \approx 23.11$ MeV if one includes the tails of the 4^+ at $E_x = 22.921$ MeV and of the 6^+ at $E_x = 23.233$ MeV. That there are two 4^+ resonances is apparent in Fig. 3 at $\theta_{\text{c.m.}} = 83.6°$ around $E_\alpha = 16.5$ MeV. Although several groups[13,33,34,40] reported a resonance near the lower 4^+, the only assignments were by Voit *et al.*[13] and James and Fletcher,[40] who claim a 6^+ around $E_x = 22.98-9$ MeV. The exit channels were α_6 and ^{8}Be, respectively. I see no evidence for a 6^+ state in the α_0 channel.

J. Energy region from $E_x = 23.19$ to 23.68 MeV

To achieve a $\chi^2/N = 1.72$ required two 6^+ and three 8^+ resonances and a possible (0^+); see Table I. The last two 8^+'s are the narrowest resonances ($\Gamma \approx 30$ keV) which I have definitely identified. The low cross section in Figs. 2–4 at $\theta_{\text{c.m.}} \approx 23°$, 46°, 76°, and 104° around $E_x = 23.23$ MeV ($E_\alpha = 16.71$ MeV) results from $P_6 \approx 0$ at these angles. The 8^+ at $E_x = 23.416$ MeV produces no structure at $E_\alpha = 16.93$ MeV in Fig. 2 at $\theta_{\text{c.m.}} = 15.4°$ near the 16.2° zero of P_8 and at $\theta_{\text{c.m.}} = 38.2°$ near the 37.2° zero of P_8; at angles intermediate to these, it appears as an interference dip in the cross section.

Figure 14 shows a $\chi^2/N = 1.26$ fit over the more restricted region from $E_x = 23.49$ to 23.68 MeV. This fit involved only the two narrowest 8^+'s at $E_x = 23.545$ and 23.623 MeV and the broad 6^+ at $E_x = 23.601$ MeV. Trying different J's for the 6^+ increased the χ^2/N to 1.57 for 0^+ and to 2.42 for 4^+. Note that the two narrow 8^+ resonances vanish at 15.4° [$P_8(16.2°) = 0$] and 100.8° [$P_8(100.6°) = 0$]. The eight minima in the angular distribution at $E_\alpha = 17.175$ MeV in Fig. 5 arise from the 8^+ at $E_x = 23.623$ MeV. Although no group previously resolved the narrow 8^+ resonances, both Andritsopoulos *et al.*[34] and Erb *et al.*[33] report resonance parameters which could correspond to one or both of the 8^+'s, and in Ref. 34 the Legendre fits indicated 8^+. In addition, Erb *et al.*[33] saw a resonance whose $E_x = 23.26$ MeV and $\Gamma \approx 125$ keV almost certainly corresponds to the lower 6^+. If this is the case, this 80 mb total cross section implies $\Gamma_c \geq 50$ keV.

K. Energy region from $E_x = 23.66$ to 23.97 MeV

Figure 15 shows a $\chi^2/N = 1.43$ fit at sample angles. The fit mainly needed only two new resonances, an 8^+ at $E_x = 23.763$ MeV and a 6^+ at $E_x = 23.819$ MeV, but also included a very weak narrow 8^+ at $E_x = 23.78$ MeV which improved the χ^2 marginally, so it is listed in parenthesis in Table I. (The tail of the 6^+ at $E_x = 23.601$ MeV also was used.) The $\theta_{\text{c.m.}} = 23.1°$ angle (Fig. 15) is near $P_6 = 0$ and hence well displays the strong 8^+ and shows a fluctuation at $E_x = 23.78$ MeV which may arise from the weak narrow 8^+. The 6^+ state contribution is also very small at $\theta_{\text{c.m.}} = 45.8°$ [$P_6(48.6°) = 0$] and $\theta_{\text{c.m.}} = 74.6°$ [$P_6(76.2°) = 0$]. Conversely, to see the 6^+ state's contribution most clearly, look at $\theta_{\text{c.m.}} = 15.4°$ [$P_8(16.2°) = 0$], and it appears as an interference dip at $\theta_{\text{c.m.}} = 60.4°$, [$P_8(58.3°) = 0$], $\theta_{\text{c.m.}} = 81.4°$ [$P_8(79.4°) = 0$], and $\theta_{\text{c.m.}} = 100.7°$ [$P_8(100.6°) = 0$]. The strong 8^+ was first assigned in 1976 by Erb *et al.*[10] but their $\Gamma = 125$ keV exceeds the present $\Gamma = 68 \pm 16$ keV. However, Erb *et al.*,[33] from excitation functions of gamma decays, quote $\Gamma = 100$ keV. Their larger widths may have arisen from including the unresolved narrow 8^+ and possibly some effects from the broad higher energy 6^+ at $E_x = 23.819$ MeV. Voit *et al.* also support the 8^+ assignment. James and Fletcher,[40] using the ^{12}C(^{12}C,^{8}Be)^{16}O(g.s.) reaction, observed a 6^+ at $E_x = 23.91$ MeV of width $\Gamma = 200$ keV. The spin assignment was based on a Legendre fit to the data. Both their width and resonant energy are sufficiently different from the 6^+ at $E_x = 23.819$ MeV that we are not likely seeing the same resonance.

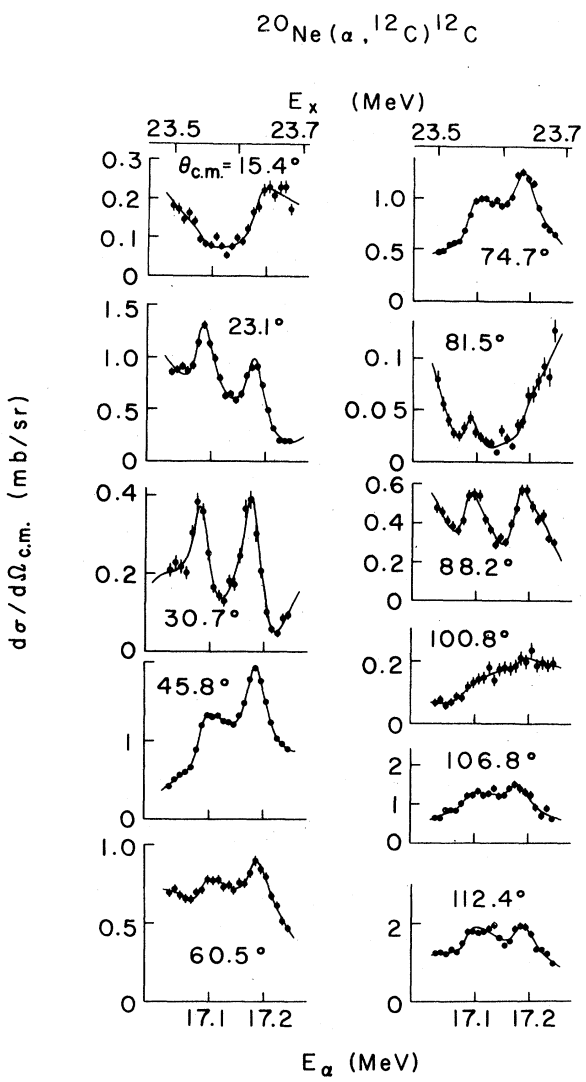

FIG. 14. Sample fits for $E_x=23.49$ to 23.68 MeV. A $\chi^2/N=1.26$ involved only three resonances at $E_x=23.545$ MeV (8^+, 3.6%, 30 keV); $E_x=23.601$ MeV (6^+, 3.7%, 188 keV); and $E_x=23.623$ MeV (8^+, 6.4%, 36 keV).

L. Energy region from $E_x=23.97$ to 24.35 MeV

I have failed to achieve any decent fits in this region. As in the energy region from $E_x=20.80$ to 21.22 MeV, this failure suggests that the structure in Figs. 2–4 arises from many overlapping resonances of comparable strength. The total cross section is low and devoid of structure. James and Fletcher[40] observed an 8^+ at $E_x=24.23$ MeV which was approximately 200 keV in width in the $^{12}C(^{12}C,^{8}Be)^{16}O$ reaction.

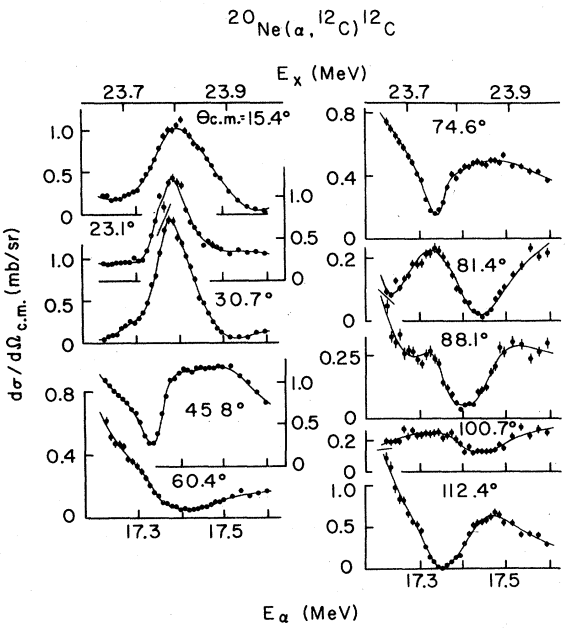

FIG. 15. Sample fits for $E_x=23.66-23.97$ MeV. A $\chi^2/N=1.43$ involved three resonances at $E_x=23.763$ MeV (8^+, 4.1%, 68 keV); $E_x=(23.78)$ MeV [(8^+), (1%), (25) keV]; and $E_x=23.819$ MeV (6^+, 4%, 135 keV), plus the tail of the broad 6^+ at $E_x=23.601$ MeV.

M. Energy region from $E_x=24.35$ to 24.83 MeV

Figure 16 shows a $\chi^2/N=1.41$ fit at several sample angles. Three 8^+ resonances dominate the fit but a 4^+ and a possible (6^+) (see Table I) were also included. Note that in Fig. 16 at $\theta_{c.m.}=81.0°$ and 100.2° one is near zeros of P_8 (79.4° and 100.6°), and the three 8^+ resonances almost vanish. Likewise at $\theta_{c.m.}=30.5°$ near a P_4 zero, the 4^+ at $E_x=24.607$ MeV disappears. The 6^+ at $E_x=24.44$ MeV is most visible at $\theta_{c.m.}=52.8°$, 81°, and 94° and is absent at $\theta_{c.m.}=22.9°$, 74.2°, and 100.2°. The latter angles are near zeros of P_6: 21.2°, 76.2°, and 103.8°. The assignment of the strongest 8^+ resonance dates back to Kuehner *et al.*[6] in 1963 and was confirmed recently by Erb *et al.*[10] and Voit *et al.*,[13] although all three quote an E_x some 30–70 keV higher than I found. Kuehner *et al.*[6] also reported a possible 8^+ at $E_x=24.68$ MeV which corresponds to the 8^+ at $E_x=24.653$ MeV. While James and Fletcher[40] in the ^{8}Be channel saw an 8^+ at $E_x=24.55$ MeV, their 300 keV width implies poor resolution or a different level. Voit *et al.*[13] in the α_6 channel claim another 8^+ at $E_x=24.83$ MeV which, however, is absent in α_0 channel of the present work.

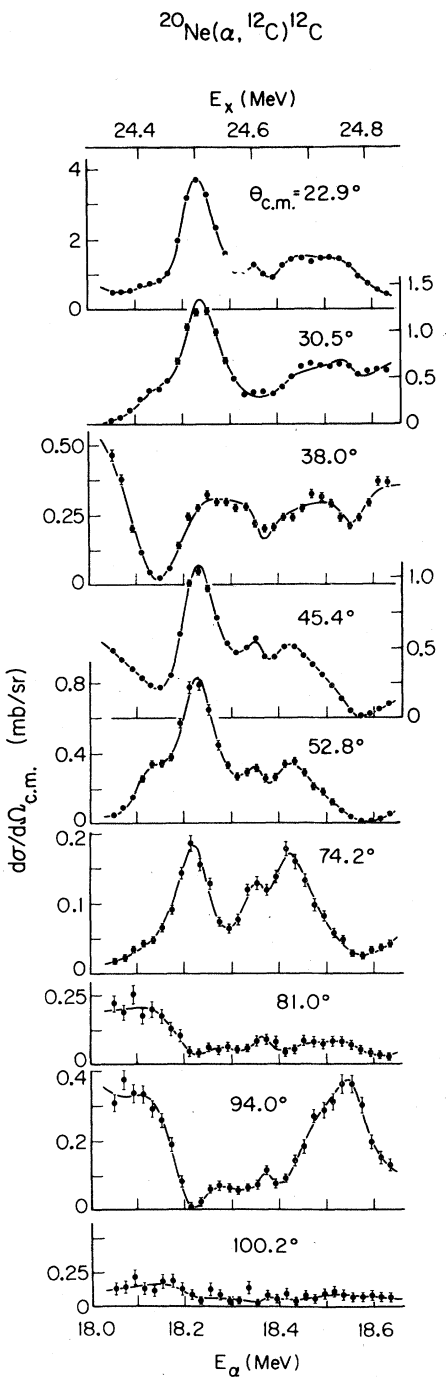

FIG. 16. Sample fits for $E_x=24.35-24.83$ MeV. A $\chi^2/N=1.41$ included five resonances at $E_x\approx24.44$ MeV [(6^+), $\sim3.5\%$, ~140 keV]; $E_x=24.490$ MeV (8^+, 9.7%, 80 keV); $E_x=24.607$ MeV (4^+, 5.0%, 40 keV); $E_x=24.653$ MeV (8^+, 7.4%, 128 keV), and $E_x=24.768$ MeV (8^+, 3.7%, 61 keV).

N. Energy region from $E_x=24.86$ to 25.44 MeV

Figure 17 shows a $\chi^2/N=1.83$ fit at several sample angles. Although the strong 8^+ resonance at $E_x=25.328$ MeV dominates, the fit required also two 6^+'s, another 8^+, and the first 10^+ resonance (see Table I). The 6^+ and 10^+ resonances show most clearly at $\theta_{c.m.}=38.0°$, where one is near a zero of P_8 (37.2°). Note the very small cross section at $\theta_{c.m.}=80.9°$, an angle which is near a zero for $P_{10}(81.4°)$, $P_8(79.4°)$, and $P_6(76.2°)$. Quite clearly there is little strength in $L=0$, 2, or

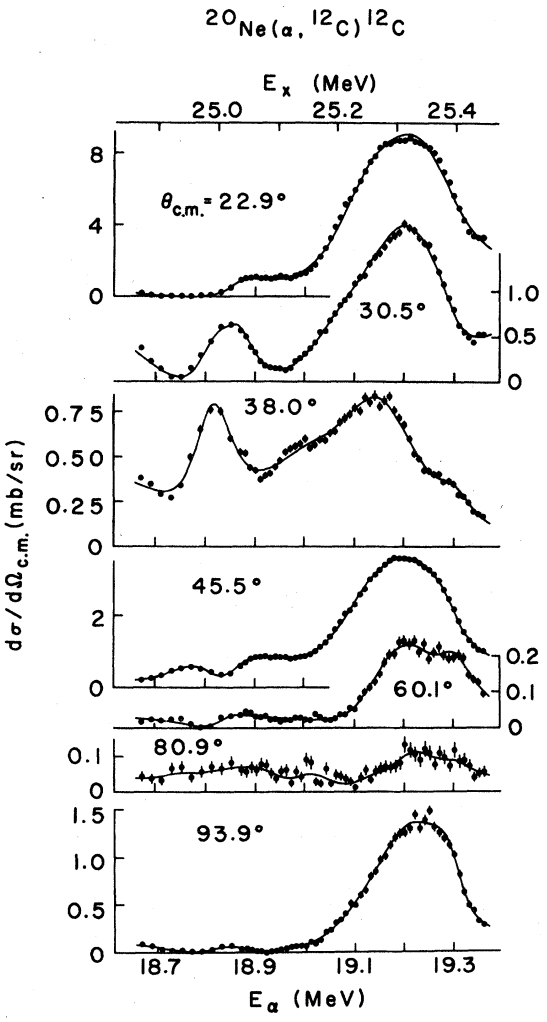

FIG. 17. Sample fits for $E_x=24.86-25.44$ MeV. A $\chi^2/N=1.83$ included five resonances at $E_x=24.983$ MeV (6^+, 4.2%, 89 keV); $E_x=25.025$ MeV (8^+, 3.2%, 72 keV); $E_x=25.244$ MeV (10^+, 3.1%, 150 keV); $E_x=25.328$ MeV (8^+, 14.2%, 202 keV), and $E_x=25.383$ MeV (6^+, 2.4%, 73 keV).

4 partial waves. The assignment for the strong 8^+ resonance dates from 1963.[4,6] The level parameters of Kuehner *et al.*[6] agree with the present ones, but Lassen and Olsen[4] claim a much smaller width (145 keV vs 202 ± 16 keV). They varied the cyclotron beam energy by putting absorbers in the beam path. More recently several groups[13,15,39–41] confirmed the assignment and generally gave parameters consistent with those of the present work. The exception is Cindro *et al.*[39] who report an E_x some 200 keV less and a width 50% larger. James and Fletcher[40] via $^{12}C(^{12}C,^{8}Be)^{16}O$ also claim a tentative 6^+, $\Gamma<450$ keV at $E_x=25.13$ MeV, but their E_x is higher enough (~150 keV) than the $E_x=24.983$ MeV of the 6^+ level correspondence may be doubtful.

O. Energy region from $E_x=25.48$ to 25.89 MeV

A $\chi^2/N=1.10$ fit over the region $E_x=25.48-25.71$ MeV required only a 6^+ at $E_x=25.563$ MeV and an 8^+ at $E_x=25.619$ MeV. The region from $E_x=25.68$ to 25.91 MeV has a structure that is much harder to pin down. There is apparently a weak (8^+) at $E_x=25.817$ MeV but I could not distinguish between a weak (8^+) or (10^+) resonance at $E_x=25.744$ MeV, since the $\chi^2/N=1.20$ for the (8^+) and 1.18 for the (10^+). The main contributions must be from wider levels which the fitting program includes as background. Fletcher *et al.*[41] report a possible 8^+ at $E_x=25.71$ MeV in the $^{12}C(^{12}C,^{8}Be)^{16}O$ reaction and James and Fletcher[40] claim an 8^+ at $E_x=25.83$ MeV of width $\Gamma=500$ keV in the same reaction. They note that there is some evidence of overlapping structure, but it is not clear that we see the same levels.

P. Energy region from $E_x=25.89$ to 26.49 MeV

Figure 18 shows a $\chi^2/N=1.16$ fit at several sample angles. The fit corresponds to three relatively strong unobscured 10^+ levels plus two 8^+ levels (see Table I). (If the fitting region is restricted to $E_x=25.89-26.14$ MeV, the lowest 8^+ and 10^+ give a $\chi^2/N=0.89$.) The $\theta_{c.m.}=30.4°$ data (Fig. 18) is near a zero of $P_{10}(30.1°)$ and thus reveals the position of the two 8^+ levels. Likewise the $\theta_{c.m.}=37.9°$ data which is near the 37.2° zero of P_8 displays clearly the three 10^+ resonances. Note also the small cross section at $\theta_{c.m.}=80.5°$

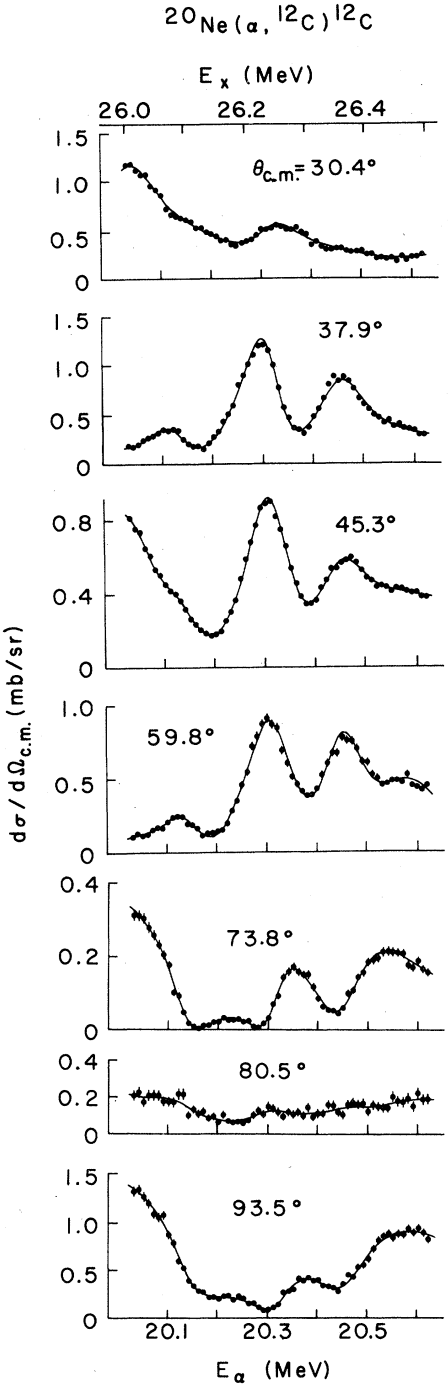

FIG. 18. Sample fits for $E_x=26.00$ to 26.49 MeV. A $\chi^2/N=1.16$ resulted from five resonances at $E_x=26.004$ MeV (8^+, 3.7%, 81 keV) (just at the border of the region but well fit in an overlapping region, see text); $E_x=26.083$ MeV (10^+, 2.4%, 65 keV); $E_x=26.230$ MeV (10^+, 7.4%, 85 keV); $E_x=26.239$ MeV (8^+, 4.5%, 106 keV), and $E_x=26.351$ MeV (10^+, 6.3%, 118 keV).

which is near both a P_8 zero (80.2°) and a P_{10} zero (81.4°). None of the five resonances correspond to previously reported states[6,40,41] with the possible exception of the claim of Kuehner *et al.*'s[6] of 10^+ strength around $E_x \approx 26.3$ MeV. The two 8^+ resonances reported[40,41] in the $^{12}C(^{12}C,^{8}Be)^{16}O$ reaction are too broad ($\Gamma \sim 200-300$ keV) to correspond to resonances reported here.

VI. SUMMARY AND CONCLUSIONS

Table I and Fig. 19 summarize the 55 levels in ^{24}Mg and their parameters which I have extracted from the data on $^{20}Ne(\alpha,^{12}C)^{12}C$. All but ten of the 55 levels are either new or previously unassigned. Only 11 of the levels and assignments I regard as sufficiently uncertain to list in parenthesis. The data also revealed large disagreements (300—40%) with earlier absolute cross sections.

The method of fitting the cross section data is not sensitive to levels with widths comparable to the fitting regions, since such broad states become indistinguishable from the linear background terms. However, the generally good χ^2/N over most of the fitted regions suggests that I have identified most of the significant narrow structure.

Some systematics of the levels merit comment. Figure 19 (and also the Legendre coefficients, Fig. 7) show that levels of each J^π appear to have both a threshold E_x and a high energy cutoff for appreciable strength. The E_x energy interval over which a particular J^π is most important seems to be ≈ 4 MeV. Such structure implies lifetimes comparable to the transit time for one carbon nucleus to pass

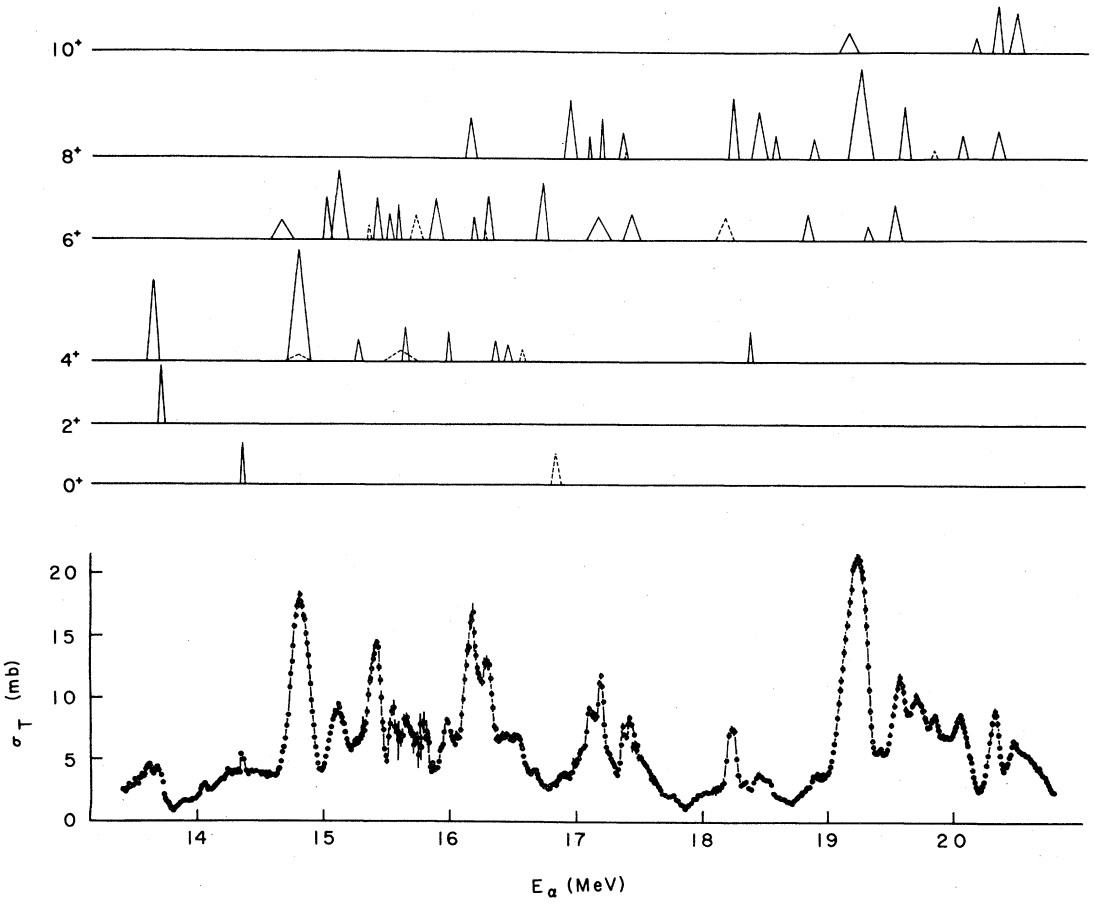

FIG. 19. Total cross section and level systematics. The position of each triangle corresponds to the energy of the resonance, the base corresponds to the width, and the height corresponds to the strength, $(\Gamma_\alpha\Gamma_c)^{1/2}/\Gamma$. Triangles with broken lines are uncertain assignments.

another and suggests very broad doorway states. The widths and positions for each such broad doorway resonance are consistent with the barrier top resonances with strong absorption in the interior which Friedman *et al.*[42,43] have suggested as important for the $^{12}C+^{12}C$ system. Barrier top or "orbiting" resonances have an energy just at the top of the centrifugal-Coulomb barrier and have their wave functions localized at the radius of the top of the barrier. This result is opposed to the concept of the "quasimolecular" resonance which arises from the potential well that is inside the barrier. Each of these broad states must then lead through alpha cluster states, some of them quite narrow, to the $^{20}Ne+\alpha$ channel.

Finally, I have obtained excitation functions of elastic and inelastic scattering of alphas from ^{20}Ne. Each channel shows a great deal of structure becoming broader and more overlapping at higher energies, but the data do not seem to be strongly correlated with the channel for symmetric fission into two ^{12}C's.

ACKNOWLEDGMENTS

I would like to express my gratitude to Professor Hugh T. Richards for his assistance, guidance, and discussions concerning this work. I also would like to thank Professor William Friedman for his explanation of barrier top resonances. The acquisition of the data was only possible with the assistance of Dr. James H. Billen, Dr. Lawrence L. Ames, S. R. Riedhauser, and G. Caskey. This work was supported in part by the United States Department of Energy.

---

*Present address: TRIUMF Laboratory, Vancouver, B.C., Canada V6T 2A3.

[1]D. A. Bromley, J. A. Kuehner, and E. Almqvist, Phys. Rev. Lett. 4, 365 (1960).
[2]E. Almqvist, D. A. Bromley, and J. A. Kuehner, Phys. Rev. Lett. 4, 515 (1960).
[3]N. O. Lassen, Phys. Lett. 1, 65 (1962); 1, 161 (1962).
[4]N. O. Lassen and J. S. Olsen, K. Dan. Vidensk. Selsk. Mat. Fys. Medd. 33, No. 13 (1963).
[5]E. Almqvist, D. A. Bromley, J. A. Kuehner, and B. Whalen, Phys. Rev. 130, 1140 (1963).
[6]J. A. Kuehner, J. D. Prentice, and E. Almqvist, Phys. Lett. 4, 332 (1963).
[7]J. Borggreen, B. Elbek, and R. B. Leachman, K. Dan. Vidensk. Selsk. Mat. Fys. Medd. 34, No. 9 (1964).
[8]E. Almqvist, J. A. Kuehner, D. McPherson, and E. W. Vogt, Phys. Rev. 136, B84 (1964).
[9]Z. Basrak, F. Auger, B. Fernandez, J. Gastebois, and N. Cindro, J. Phys. (Paris) Lett. 37, L131 (1976).
[10]K. A. Erb, R. R. Betts, D. L. Hanson, M. W. Sachs, R. L. White, P. P. Tung, and D. A. Bromley, Phys. Rev. Lett. 37, 670 (1976).
[11]Z. Basrak, F. Auger, B. Fernandez, J. Castebois, and N. Cindro, Phys. Lett. 65B, 119 (1976).
[12]W. Galster, W. Treu, P. Dück, H. Fröhlich, and H. Voit, Phys. Rev. C 15, 950 (1977); Phys. Lett. 67B, 262 (1977).
[13]H. Voit, W. Galster, W. Treu, H. Fröhlich, and P. Dück, Phys. Lett. 67B, 399 (1977).
[14]F. Coçu, N. Cindro, J. Uzureau, Z. Basrak, M. Cates, J. M. Fieni, E. Holub, Y. Patin, and S. Plattard, Fizika (Zagreb) 9, Supp. 2, 26 (1977).
[15]W. Treu, H. Fröhlich, W. Galster, P. Dück, and H. Voit, Phys. Rev. C 18, 2148 (1978).
[16]E. R. Cosman, R. Ledoux, and A. J. Lazzarini, Phys. Rev. C 21, 2111 (1980).
[17]W. Galster, P. Dück, H. Fröhlich, W. Treu, H. Voit, and S. M. B. Lee, Phys. Rev. C 22, 515 (1980).
[18]R. G. Stokstad, in *Europhysics Study Conference on Intermediate Processes in Heavy Ion Reactions, Plitvice,* edited by N. Cindro, P. Kulisic, and Meyer-Kuckuk (Springer, Berlin, 1972).
[19]C. Kalbach, Nukleonik 19, 117 (1974).
[20]H. Feshbach, J. Phys. 37, Coll. C5, Supp. 11, 177 (1976).
[21]D. A. Bromley, in *Nuclear Molecular Phenomena,* edited by N. Cindro (North-Holland, Amsterdam, 1978); in *Nuclear Reactions Induced by Heavy Ions,* edited by R. Bock and W. R. Hering (American Elsevier, New York, 1970).
[22]P. E. Hodgson, in *Nuclear Heavy Ion Reactions* (Oxford University, New York, 1978).
[23]K. A. Erb and D. A. Bromley, Phys. Today 32, No. 1, 34 (1979).
[24]C. A. Davis, Ph. D. thesis, University of Wisconsin, 1981 (unpublished).
[25]J. H. Billen, Ph.D. thesis, University of Wisconsin, 1978 (unpublished), available through University Microfilms, Inc., Ann Arbor, Michigan; J. H. Billen, Phys. Rev. C 20, 1648 (1979).
[26]D. A. Bromley (private communication). The data is presented in corrected form in Ref. 23.
[27]H. Voit (private communication).
[28]R. Abegg and C. A. Davis (to be published).
[29]O. Haüsser, T. K. Alexander, D. L. Disdier, A. J. Ferguson, A. B. McDonald, and I. S. Towner, Nucl. Phys. A216, 617 (1973).
[30]S. K. Korotky, K. A. Erb, S. J. Willett, and D. A. Bromley, Phys. Rev. C 20, 1014 (1979).
[31]K. C. Young, Jr., R. W. Zurmuhle, J. M. Lind, and

D. P. Balamuth, Nucl. Phys. A330, 477 (1979).
[32]A. Gobbi, P. R. Maurenzig, L. Chua, R. Hadsell, P. D. Parker, M. W. Sachs, D. Shapira, R. Stokstad, R. Wieland, and D. A. Bromley, Phys. Rev. Lett. 26, 396 (1971).
[33]K. A. Erb, R. R. Betts, S. K. Korotky, M. M. Hindi, P. P. Tung, M. W. Sachs, S. J. Willett, and D. A. Bromley, Phys. Rev. C 22, 507 (1980).
[34]G. Andritsopoulos, X. Aslanoglou, P. Bakoyeorgos, and G. Vourvopoulos, Phys. Rev. C 21, 1648 (1980).
[35]E. R. Cosman, T. M. Cormier, K. van Bibber, A. Sperduto, G. Young, J. Erskine, L. R. Greenwood, and Ole Hansen, Phys. Rev. Lett. 35, 265 (1975).
[36]K. van Bibber, E. R. Cosman, A. Sperduto, T. M. Cormier, T. N. Chin, and Ole Hansen, Phys. Rev. Lett. 32, 687 (1974).
[37]A. M. Sandorfi and A. M. Nathan, Phys. Rev. Lett. 40, 1252 (1978).
[38]E. Kuhlmann, E. Ventura, J. R. Calarco, D. G. Mavis, and S. S. Hanna, Phys. Rev. C 11, 1525 (1975).
[39]N. Cindro, F. Coçu, J. Uzureau, Z. Basrak, M. Cates, J. M. Fieni, E. Holub, Y. Patin, and S. Plattard, Phys. Rev. Lett. 39, 1135 (1977).
[40]D. R. James and N. R. Fletcher, Phys. Rev. C 17, 2248 (1978).
[41]N. R. Fletcher, J. D. Fox, G. J. KeKelis, G. R. Morgan, and G. A. Norton, Phys. Rev. C 13, 1173 (1976).
[42]W. A. Friedman, K. W. McVoy, and M. C. Nemes, Phys. Lett. 87B, 179 (1977).
[43]W. A. Friedman and C. J. Goebel, Ann. Phys. (N.Y.) 104, 145 (1977).
[44]See AIP document No. PAPS PRVCA-24-1891-244 for 244 pages of differential cross sections and Legendre coefficients. Order by PAPS number and journal reference from American Institute of Physics, Physics Auxiliary Publication Service, 335 East 45th Street, New York, N.Y. 10017. The price is $4.50 microfiche or $37.10 for photocopies. Make checks payable to American Institute of Physics.